

Quantum-enhanced mean value estimation via adaptive measurement

Kaito Wada,^{1,*} Kazuma Fukuchi,¹ and Naoki Yamamoto^{1,2}

¹*Department of Applied Physics and Physico-Informatics, Keio University,
3-14-1 Hiyoshi, Kohoku-ku, Yokohama, Kanagawa, 223-8522, Japan*

²*Quantum Computing Center, Keio University, 3-14-1 Hiyoshi,
Kohoku-ku, Yokohama, Kanagawa, 223-8522, Japan*

Estimating the mean values of quantum observables is a fundamental task in quantum computing. In particular, efficient estimation in a noisy environment requires us to develop a sophisticated measurement strategy. Here, we propose a quantum-enhanced estimation method for the mean values, that adaptively optimizes the measurement (POVM); as a result of optimization, the estimation precision gets close to the quantum Cramér-Rao lower bound, that is, inverse of the quantum Fisher information. We provide a rigorous analysis for the statistical properties of the proposed adaptive estimation method such as consistency and asymptotic normality. Furthermore, several numerical simulations with large system dimension are provided to show that the estimator needs only a reasonable number of measurements to almost saturate the quantum Cramér-Rao bound.

I. INTRODUCTION

The mean value estimation of quantum observables is an important subroutine in many quantum algorithms for both near-term noisy and future fault-tolerant quantum devices. Especially, variational quantum algorithms, which have been studied extensively in recent years [1–13], require estimating mean values iteratively to train the variational parameters on a parameterized quantum circuit. However, typically when the target observable is a molecular Hamiltonian as in the variational quantum eigensolver [2, 14], the standard estimation method needs astronomically many measurements [14–17], and thus any possible quantum advantage may be lost. In addition, real quantum devices suffer from noise induced by the interaction of system and environment, and such noise deteriorates the efficiency for reading out calculation results. Therefore, developing efficient mean-value estimation methods in a noisy environment is highly important [17, 18].

For this purpose, the statistical estimation theory [19, 20] is of course useful. Actually its quantum extension, the statistical quantum estimation theory, has been established [21, 22]. In particular, the seminal Cramér-Rao inequality and Fisher information, which can be used to characterize the limit of estimation precision, has been extended to quantum settings [22–26]. This result, known as the quantum Cramér-Rao (QCR) inequality and quantum Fisher information, plays a practically important role in many applications such as quantum sensing [27] and, further, reveals some fundamental limitation on information extractable from quantum mechanical systems [28].

Hence the statistical quantum estimation theory could be effectively applied to improve estimation efficiency of subroutines in quantum computing. However, such exploration has just started. For instance, some

less-demanding implementation methods for quantum-enhanced (i.e., less query complexity compared to any classical means) amplitude estimation algorithm have been proposed and their performance were investigated in depth using statistical estimation theory, yet without studying QCR bound [29–34]. To our best knowledge, only Ref. [35] provides a quantum-enhanced amplitude estimation method that asymptotically achieves the QCR bound when several conditions are satisfied in a noisy environment.

Moreover, we recently find the quantum-enhanced mean value estimation method [18] that utilizes techniques from the quantum signal processing (QSP) [36]. This method employs QSP-inspired parameterized quantum circuits and executes the Bayesian inference for the target value based on the result of a fixed measurement on the parameterized quantum circuits. The key point for efficient estimation is that the variance of the posterior distribution can be rapidly decreased by adjusting the parameters of the quantum circuit in each measurement. However, this method does not consider optimizing the measurement for better estimation and no statistical guarantee of the estimator to hit the true mean value was provided. Importantly, Ref. [17] provided a benchmark using the same Bayesian inference, which clarifies the need for more efficient estimation method to achieve quantum advantage. Hence it is of increasing attraction to develop an algorithm that possibly achieves the QCR bound.

In this paper, we propose a new quantum-enhanced mean-estimation method that asymptotically achieves QCR bound with some provable statistical properties. This method uses a modified maximum likelihood estimation that incorporates an adaptive optimization based on the Fisher information. More precisely, this scheme adjusts the number of amplitude amplification operations and the measurement (more precisely POVM), which as a result enables the estimator to almost achieve the QCR bound as the number of qubits increases. As in the previous study [18, 35, 37], we employ the depolarizing channel as a noise model. As pointed out in the previous

* wkai1013keio840@keio.jp

study, the quantum mean value estimation under the depolarizing noise may significantly deteriorate depending on the target value to be estimated, but we will numerically demonstrate that the proposed method can also get around the problem due to the optimization. In addition, we prove that the estimator satisfies the following statistical properties.

- Consistency: As the number of measurements increases, the estimation accuracy becomes better. More precisely, the probability that the estimated value is identical to the true value approaches 1, which is clearly a desirable statistical property.
- Asymptotic normality: For the target value, the estimator regularized by its Fisher information follows the standard normal distribution and as a result the estimation error asymptotically achieves the Cramér-Rao lower bound, as the number of measurements increases. Note that this property corresponds to the central limit theorem that holds for usual methods for estimating the quantum mean value in quantum computing.

These asymptotic properties guarantee the quality of our estimates, and we will also demonstrate that these properties hold even for a practical number of measurements.

This article is organized as follows. In Section II, we review the maximum likelihood amplitude estimation algorithm and show the estimation precision of this algorithm deteriorates in the presence of depolarizing noise. In Section III, we propose a new quantum mean value estimation method with adaptive measurements. We first introduce two-type measurements (POVMs) and construct our algorithm with optimization for efficient estimation. Next, we show some statistical properties of our method. Section IV is devoted to show the results of numerical simulations and discussion. Finally, we conclude this paper in Section V.

II. PRELIMINARY

The (quantum-enhanced) amplitude estimation algorithm studied in [35, 37–39], which does not use the hard-to-implement phase estimation algorithm, consists of two major steps. The first step is to perform amplitude amplification on the quantum state whose amplitude is to be estimated, and then make a measurement; this procedure is repeated with different operation times. The second step is to estimate the amplitude by classical post-processing for the combined measurement result, i.e., the maximum likelihood estimation.

The problem is to estimate the amplitude $\sin(\phi^*)$, with unknown $\phi^* \in [0, \pi/2]$, of the following $(n+1)$ -qubit quantum state $\mathcal{A}|0\rangle_{n+1}$:

$$\mathcal{A}|0\rangle_{n+1} := \cos(\phi^*)|\psi_0\rangle_n|0\rangle_1 + \sin(\phi^*)|\psi_1\rangle_n|1\rangle_1, \quad (1)$$

where $|0\rangle_{n+1}$ is the computational basis of $(n+1)$ -qubit. Here, \mathcal{A} is a unitary operator whose action is defined

as Eq. (1), and $|\psi_0\rangle_n$ and $|\psi_1\rangle_n$ are normalized n -qubit quantum states. The first step is to amplify the amplitude via the operator \mathcal{Q} defined as

$$\mathcal{Q} := \mathcal{A}(2|0\rangle_{n+1}\langle 0|_{n+1} - I_{n+1})\mathcal{A}^\dagger(I_n \otimes Z), \quad (2)$$

where I_n is the identity operator on the n -qubit system, and Z denotes the 2×2 Pauli Z matrix. When \mathcal{Q} is applied m times to the state (1), we obtain [40]

$$\begin{aligned} \mathcal{Q}^m \mathcal{A}|0\rangle_{n+1} &= \cos[(2m+1)\phi^*]|\psi_0\rangle_n|0\rangle_1 \\ &\quad + \sin[(2m+1)\phi^*]|\psi_1\rangle_n|1\rangle_1. \end{aligned} \quad (3)$$

We now measure the last qubit of Eq. (3) by the computational basis $|0\rangle_1$ and $|1\rangle_1$. Then the probability of obtaining "1" is given by

$$\tilde{\mathbf{P}}(m; \phi^*) := \frac{1}{2} - \frac{1}{2} \cos[2(2m+1)\phi^*]. \quad (4)$$

Note that this is equivalent to the Bernoulli trials with success probability $\tilde{\mathbf{P}}(m; \phi^*)$.

In the second step we estimate the amplitude based on the measurement results obtained in the first step by the maximum likelihood estimation method. For each of predefined odd numbers $2m_k + 1$ ($k = 1, 2, \dots, M$), we prepare the state (3) and measure it N times with the computational basis independently. We write $x^{(k)} \in \{0, 1, \dots, N\}$ as the number of hitting "1" for the state $\mathcal{Q}^{m_k} \mathcal{A}|0\rangle_{n+1}$. The measurement results for M different states are put together as $\mathbf{x}_M := (x^{(1)}, x^{(2)}, \dots, x^{(M)})$. Then the likelihood function to have \mathbf{x}_M is given by

$$\tilde{\mathcal{L}}_M(\phi; \mathbf{x}_M) := \prod_{k=1}^M \tilde{F}_k(x^{(k)}; m_k, \phi), \quad (5)$$

where $\tilde{F}_k(x^{(k)}; m_k, \phi)$ is the probability of obtaining $x^{(k)}$. Given the measurements \mathbf{x}_M , the maximum likelihood estimation assumes that the value of ϕ that maximizes $\tilde{\mathcal{L}}_M(\phi; \mathbf{x}_M)$ is a plausible estimate of the true value ϕ^* . In other words, the maximum likelihood estimate $\hat{\phi}_M$ for ϕ^* from the M series of measurements is defined as

$$\hat{\phi}_M := \operatorname{argmax}_{\phi \in [0, \pi/2]} \tilde{\mathcal{L}}_M(\phi; \mathbf{x}_M). \quad (6)$$

Note that the maximum likelihood estimator for $\sin(\phi^*)$ corresponds to $\sin(\hat{\phi}_M)$ due to the invariance property of maximum likelihood estimators. Thanks to the amplitude amplification, the estimation precision of ϕ^* can be improved quadratically with respect to the number of total queries, by using a specific sequence of m_k as demonstrated in [38].

We now consider the n -qubit depolarizing channel:

$$\mathcal{D}[\rho] := p\rho + \frac{1-p}{d}I_n, \quad d := 2^n, \quad (7)$$

where ρ is an arbitrary density operator and $1-p$ is the probability that depolarization occurs. In this paper,

as in [18, 35, 37], we consider a noise model in which depolarization occurs with probability $1 - p_s$ for state preparation and $1 - p_q$ for each amplitude amplification. Then the probability of obtaining "1" for the final state under this noise model is given by

$$\tilde{\mathbf{P}}_{\mathcal{D}}(m; \phi^*) := \frac{1}{2} - \frac{p_s p_q^m}{2} \cos[2(2m+1)\phi^*]. \quad (8)$$

The subscript \mathcal{D} means that the quantum state to be measured has passed through the above-defined depolarizing channels. Then the classical Fisher information associated with the probability (8) for ϕ^* is calculated as

$$\tilde{\mathcal{I}}_c(m; \phi^*) := \frac{(2m+1)^2 (p_s p_q^m)^2 \sin^2[2(2m+1)\phi^*]}{\tilde{\mathbf{P}}_{\mathcal{D}}(m; \phi^*) (1 - \tilde{\mathbf{P}}_{\mathcal{D}}(m; \phi^*))}. \quad (9)$$

Equation (9) indicates that the estimation may become ineffective if m satisfies $\sin[2(2m+1)\phi^*] \simeq 0$. More precisely, if m and ϕ^* satisfy this condition, the Cramér-Rao lower bound of the estimation error for ϕ^* significantly deteriorates [18, 37]. In addition, even if we use the above-described maximum likelihood estimation based on the M series of measurements for m_k ($k = 1, 2, \dots, M$), which are predefined independently to ϕ^* , the same deterioration may occur [37]. Importantly, this phenomena are also seen in the quantum mean value estimation problem discussed in the next section.

III. QUANTUM-ENHANCED MEAN VALUE ESTIMATION

A. Two-way amplitude amplification

Our goal is to estimate the mean value of a Hermitian operator \mathcal{O} with eigenvalues ± 1 , i.e., $\langle \mathcal{O} \rangle := \langle A | \mathcal{O} | A \rangle$, where $|A\rangle := A |0\rangle_n$ is an n -qubit quantum state with a unitary operator A . The amplitude estimation method described in the previous section can be applied to this problem; hence, ideally, we need quadratically less queries compared to the standard algorithm without amplitude amplification, to estimate the mean value with specified estimation error — that is, the quantum-enhanced mean value estimation.

Suppose $|A\rangle$ is not an eigenstate of \mathcal{O} (thus $|\langle \mathcal{O} \rangle| \neq 1$) and that the two quantum states $|A\rangle$ and $\mathcal{O}|A\rangle$ are linearly independent and form the following subspace [18, 41]:

$$\mathcal{S} := \text{Span}\{|A\rangle, \mathcal{O}|A\rangle\} = \text{Span}\{|A\rangle, |A^\perp\rangle\}, \quad (10)$$

where $|A^\perp\rangle$ is a normalized state orthogonal to $|A\rangle$ obtained by Gram-Schmidt procedure to $|A\rangle$ and $\mathcal{O}|A\rangle$. We denote $|A\rangle$ and $|A^\perp\rangle$ as $|\bar{0}\rangle$ and $|\bar{1}\rangle$, respectively, and identify \mathcal{S} as the 1-qubit Hilbert space likewise the idea of qubitization [36]. We then define an n -qubit operator Q on \mathcal{S} , which corresponds to the amplitude amplification operator in Eq. (2), as

$$Q := A(2|0\rangle_n \langle 0|_n - I_n) A^\dagger \mathcal{O}. \quad (11)$$

This operator keeps the subspace \mathcal{S} invariant. Now the representation of Q on \mathcal{S} is expressed as $Q|_{\mathcal{S}} = R_{\bar{Y}}(-2\theta^*)$, where \bar{Y} is the Pauli Y matrix in the basis $|\bar{0}\rangle$ and $|\bar{1}\rangle$, and $\theta^* := \arccos(\langle \mathcal{O} \rangle)$. Note that, for the target mean value $\langle \mathcal{O} \rangle = \cos\theta^*$, the domain of θ^* is given by $\theta^* \in (0, \pi)$, which is twice as that of ϕ^* in the previous section. Acting Q on $|A\rangle$ m times yields

$$\begin{aligned} Q^m |A\rangle &= (Q|_{\mathcal{S}})^m |\bar{0}\rangle \\ &= \cos(m\theta^*) |\bar{0}\rangle - \sin(m\theta^*) |\bar{1}\rangle. \end{aligned} \quad (12)$$

Here, as in the previous case, we assume that the state is subjected to the depolarization noise through the amplitude amplification process; that is, the output state after m repetition of Q is given by

$$\rho_{\mathcal{D}}(m; \theta^*) := p_s p_q^m \rho(m; \theta^*) + \frac{1 - p_s p_q^m}{d} I_n, \quad (13)$$

where $\rho(m; \theta^*) := Q^m |A\rangle \langle A| (Q^m)^\dagger$. Here, $1 - p_q (> 0)$ denotes the probability of depolarization noise occurring along the single query of the operator Q .

To best efficiently read out quantum mean values from the amplitude-amplified quantum state (13), we need a POVM whose classical Fisher information achieves the quantum Fisher information for the state; see Appendix A for a summary of this basic theory. In fact we found a 3-valued POVM that satisfies this requirement for a certain class of θ^* . Because this 3-valued POVM contains the θ^* -dependent quantum state, which cannot be directly implemented on a device, we marginalize this POVM and end up with the following 2-valued POVM:

$$\begin{aligned} M_1^{(\text{even})} &:= I_n - M_0^{(\text{even})}, \\ M_0^{(\text{even})} &:= \mathcal{O}^\dagger |A\rangle \langle A| \mathcal{O}, \end{aligned} \quad (14)$$

where the meaning of *even* is explained later. The derivation is given in Appendix B. Measuring Eq. (13) with the POVM (14), we obtain the result corresponding to $M_1^{(\text{even})}$ with probability

$$\begin{aligned} \mathbf{P}_{\mathcal{D}}^{(\text{even})}(m; \theta^*) \\ := \frac{d-1}{d} + p_s p_q^{m+1/2} \left[\sin^2[(m+1)\theta^*] - \frac{d-1}{d} \right], \end{aligned} \quad (15)$$

where $p_q^{1/2}$ denotes the additional noise associated with the implementation of A^\dagger in $M_0^{(\text{even})}$. This measurement has powerful estimation capabilities in the sense of its Fisher information, as follows. The classical Fisher information per shot with Eq. (15) can be calculated as

$$\begin{aligned} \mathcal{I}_c^{(\text{even})}(m; \theta^*) \\ := \frac{(2m+2)^2 p_s^2 p_q^{2m+1} \sin^2[(2m+2)\theta^*]}{4\mathbf{P}_{\mathcal{D}}^{(\text{even})}(m; \theta^*) (1 - \mathbf{P}_{\mathcal{D}}^{(\text{even})}(m; \theta^*))}. \end{aligned} \quad (16)$$

Also we can calculate the quantum Fisher information using the standard recipe found in e.g., [42, 43]:

$$\mathcal{I}_q^{(\text{even})}(m) := \frac{(p_s p_q^{m+1/2})^2}{\frac{2}{d} + (1 - \frac{2}{d}) p_s p_q^{m+1/2}} (2m + 2)^2. \quad (17)$$

When $\cos[(m+1)\theta^*] \neq 0$, the classical Fisher information asymptotically approaches the quantum Fisher information for some combinations of m and θ^* , in the large dimension limit $d = 2^n \rightarrow \infty$:

$$\mathcal{I}_c^{(\text{even})}(m; \theta^*) \rightarrow \mathcal{I}_q^{(\text{even})}(m). \quad (18)$$

This means that, to estimate a *particular* θ^* , the POVM (14) becomes optimal with respect to the Fisher information, as the number of qubits increases; more precise analysis is provided in Appendix B. In the next subsection, for estimating θ^* , i.e., $\langle \mathcal{O} \rangle$, we introduce a new algorithm that is optimal for *almost all* θ^* in the large system dimension by optimizing m (the number of queries of Q).

Although the even POVM (14) can become optimal in the sense of Fisher information, this does not necessarily guarantee that the actual estimator (particularly the maximum likelihood estimator based on the POVM) produces the best estimate that achieves the QCR bound. Actually, the probability (15) is an even function with respect to the value $\theta^* - \pi/2$, and the maximum likelihood estimation associated with this even POVM cannot distinguish the sign of quantum mean values. To construct an estimator that may correctly estimate the true target value, we therefore introduce the following second POVM that breaks the above-mentioned symmetry:

$$\begin{aligned} M_1^{(\text{odd})} &:= I_n - M_0^{(\text{odd})}, \\ M_0^{(\text{odd})} &:= \frac{I_n + \mathcal{O}}{2}. \end{aligned} \quad (19)$$

This POVM corresponds to Eq. (8) in the standard amplitude estimation algorithm, because the probability of obtaining "1" by measuring the state (13) with the POVM (19) is given as

$$\mathbf{P}_D^{(\text{odd})}(m; \theta^*) = \frac{1}{2} - \frac{p_s p_q^m}{2} \cos[(2m+1)\theta^*]. \quad (20)$$

The coefficient of θ^* differs by the factor 2 compared to that of ϕ^* in Eq. (8), because the presence of sign for quantum mean values doubles the domain of the target value. Since the probability (20) is an odd function unlike Eq. (15), the measurement can distinguish the sign of the target mean value. For this reason, we have added the superscript *even* or *odd* for the POVMs (14) and (19). Note that, in contrast to the even POVM, the classical Fisher information corresponding to the odd POVM, $\mathcal{I}_c^{(\text{odd})}(m; \theta^*)$, always deviates from the quantum Fisher information even if the number of qubits increases; see Appendix B. Hence, our estimator is composed of the

even and odd POVMs, where the probability of obtaining the measurement result "1" is summarized as follows:

$$\begin{aligned} \mathbf{P}_D(\alpha; \theta^*) &:= \begin{cases} \frac{1}{2} - \frac{\eta_\alpha}{2} \cos(\alpha\theta^*), & \alpha \text{ is odd} \\ \frac{d-1}{d} + \eta_\alpha \left[\sin^2\left(\frac{\alpha}{2}\theta^*\right) - \frac{d-1}{d} \right], & \alpha \text{ is even} \end{cases}. \end{aligned} \quad (21)$$

Here $\eta_\alpha = p_s p_q^{\frac{\alpha-1}{2}}$ and $\alpha \in \mathbb{N}$ represents the number of queries of the operator A or A^\dagger . We perform the measurement via Eq. (19) when α is odd and via Eq. (14) when α is even. In the following, we call α the *amplified level*. Also, the classical/quantum Fisher information corresponding to each measurement is calculated as

$$\mathcal{I}_c(\alpha; \theta^*) := \frac{\alpha^2 \eta_\alpha^2 \sin^2(\alpha\theta^*)}{4\mathbf{P}_D(\alpha; \theta^*)(1 - \mathbf{P}_D(\alpha; \theta^*))}, \quad (22)$$

$$\mathcal{I}_q(\alpha) := \frac{\alpha^2 \eta_\alpha^2}{\frac{2}{d} + (1 - \frac{2}{d}) \eta_\alpha}. \quad (23)$$

To estimate the mean value $\langle \mathcal{O} \rangle = \cos\theta^*$, we take the maximum likelihood estimation method using the two-way amplitude amplification combined with the above POVMs.

B. The proposed adaptive mean-value estimation algorithm

When $\sin(\alpha\theta^*) \simeq 0$, the classical Fisher information (22) becomes nearly zero, and thus the estimation becomes inefficient. Hence such α should be avoided, in both POVMs (14) and (19). Yet we should employ measurements whose classical Fisher information approaches the quantum Fisher information for enhancing the estimation power. Here we provide a mean value estimation method that adaptively adjusts the amplified level α and thereby satisfies the above-mentioned two requirements. Importantly, this method inherits several good properties of the maximum likelihood estimation, as proven in Section III C. Note that in the context of the standard amplitude estimation algorithms in Section II the relation similar to Eq. (18) has already known [35]. However, unlike our method, the algorithm of [35] is unable to take full advantage of this optimality due to the problem of vanishing classical Fisher information at certain points.

The general framework of our algorithm is based on the maximum likelihood estimation method for the random variables following the probability (21). An overview is shown in Fig. 1. In the following, we describe the procedure.

- (i) Before starting the estimation, identify the probabilities of depolarization $1 - p_s$ and $1 - p_q$ by some

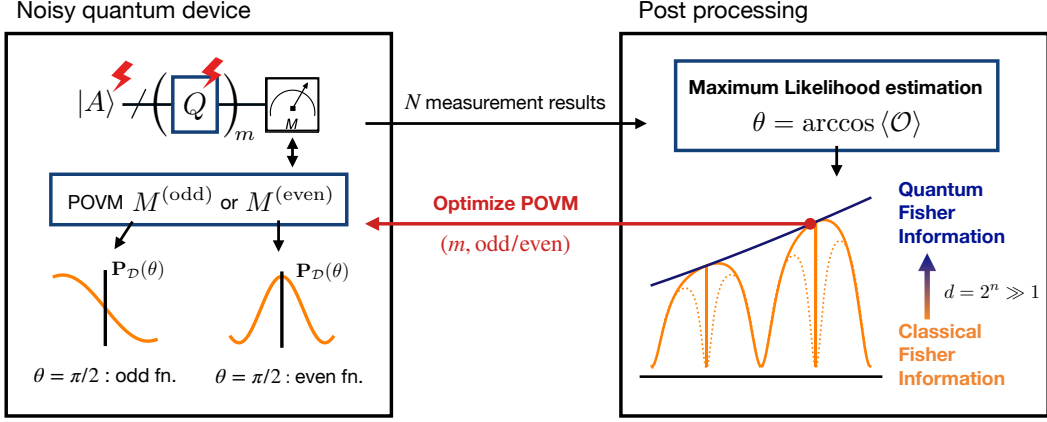


FIG. 1. Overview of the proposed algorithm for estimating $\langle \mathcal{O} \rangle = \langle A | \mathcal{O} | A \rangle$. Here, $|A\rangle$ is a target state prepared by operating an n -qubit quantum circuit A on the computational basis $|0\rangle_n$, and \mathcal{O} is a target Hermitian operator with eigenvalues ± 1 . The general framework is a modified maximum likelihood estimation method using the specific quantum circuits with the amplitude amplification operator Q and the two POVMs $M^{(\text{even})}$, $M^{(\text{odd})}$. The measurement based on the two POVMs yields probability distributions with different symmetries, and as a result the proposed algorithm can estimate the mean value $\langle A | \mathcal{O} | A \rangle$ correctly including its sign. Here, we assume the depolarization noise is induced in preparing $|A\rangle$ and querying Q . Even under this noisy condition, the algorithm can estimate the target value efficiently in the sense of the Fisher information by optimizing the number of querying Q and the POVM. In particular, optimizing every N measurements improves the classical Cramér-Rao lower bound so that it gets close to the quantum Cramér-Rao lower bound sufficiently in large system dimension d .

experiments on the quantum device to be used. For the first measurements, we set the amplified level α_1 to 1.

Unlike Bayesian estimation, our algorithm does not require any prior information on the target value.

- (ii) We measure the quantum state (13) N times independently with either POVM (14) or (19), according to the amplified level α_k . We write the total number of hitting "1" as $x^{(k)} \in \{0, 1, \dots, N\}$. Here, $x^{(k)}$ is a realization of the Binomial random variable

$$X^{(k)} \sim \text{Bin}(N, \mathbf{P}_{\mathcal{D}}(\alpha_k; \theta^*)). \quad (24)$$

- (iii) Calculate the maximum likelihood estimate $\hat{\theta}_k$ based on the total k measurement results $\mathbf{x}_k := (x^{(1)}, x^{(2)}, \dots, x^{(k)})$. Here, the estimate maximizes the following likelihood function

$$\mathcal{L}_k(\theta; \mathbf{x}_k) := \prod_{m=1}^k F_m(x^{(m)}; \alpha_m(\mathbf{x}_{m-1}), \theta), \quad (25)$$

where $F_m(x^{(m)}; \alpha_m(\mathbf{x}_{m-1}), \theta^*)$ is the probability function of random variable $X^{(m)}$.

Note that the measurements \mathbf{x}_k collect the already obtained results via measurements with α_m ($m = 1, 2, \dots, k$). Since the amplified level α_k depends on the previous results \mathbf{x}_{k-1} as described below, the likelihood function $\mathcal{L}_k(\theta; \mathbf{x}_k)$ has a hierarchical structure, which does not appear in Eq. (5).

- (iv) To enhance the classical Fisher information, we determine α_{k+1} for the next measurement based on the current estimate $\hat{\theta}_k$ by numerically solving the following optimization problem

$$\alpha_{k+1} := \underset{\alpha \in D_k}{\text{argmax}} \mathcal{I}_c(\alpha; \hat{\theta}_k) \left| \sin(\alpha \hat{\theta}_k) \right|^\delta, \quad (26)$$

where $D_k \subset \mathbb{N}$ is the range of α_{k+1} to be optimized. Once $(k+1)$ -th amplified level α_{k+1} is determined, return to (ii) and perform the measurement again.

Here, $|\sin(\alpha \hat{\theta}_k)|^\delta$ is a regularization term to avoid instability of the numerical optimization, which comes from the discontinuity of $\mathcal{I}_c(\alpha; \theta)$ (See Appendix B). In this paper, we use $\delta = 0.10$. Note that, since the elements of D_k are integer, the optimization problem can be solved fast. Importantly, this optimization has a role of not only selecting an optimal α for large Fisher information but also controlling the following trade-off by setting the optimization range of each α_{k+1} . A large α is preferred to enhance the Fisher information per 1 shot, but if we choose an α which dramatically (e.g., super-exponentially) increases with respect to m , the estimation will be failed in practical N because the likelihood function $\mathcal{L}_k(\theta; \mathbf{x}_k)$ has many peaks around the true target value. Note that the objective function $\mathcal{I}_c(\alpha; \hat{\theta}_k)$ has another trade-off between the number of querying Q and the effect of noise induced by Q ; thus the maximum number of querying Q i.e., amplified level, is also bounded by the noise levels of the quantum devices if we employ $D_k \subseteq D_{k+1} \forall k$. This means that the algorithm can perform the estimation of quantum mean values by best use of the noisy quantum devices.

C. Statistical properties of our estimator

Although the random variables $X^{(k)}$ describing the measurement results are dependent with each other and have the hierarchical structure in Eq. (25), we can prove the consistency of our estimator based on the convergence of α_k , which intuitively means that these random variables become independent with each other in large N .

Theorem 1. (Consistency; informal version.) *There exists a unique maximum likelihood estimator $\hat{\theta}_M$ of $\mathcal{L}_M(\theta; \mathbf{X}_M)$ such that*

$$\cos \hat{\theta}_M \rightarrow \langle \mathcal{O} \rangle, \quad (27)$$

as $N \rightarrow \infty$. In addition, $\alpha_k(\mathbf{X}_{k-1})$ converges to a constant α_k^* in the sense of probability as follows

$$\lim_{N \rightarrow \infty} P[\alpha_k(\mathbf{X}_{k-1}) = \alpha_k^*] = 1, \quad k = 2, \dots, M, \quad (28)$$

where $\alpha_k(\mathbf{x}_{k-1})$ denotes the optimized amplified level based on the measurement results \mathbf{x}_{k-1} . The explicit form of α_k^* is provided in Appendix C.

This theorem shows that our estimator is valid in the sense that more data gives more accurate estimation. That is, unlike the previous method [18] which uses Bayesian inference based on the measurement with the odd POVM (19) (NOT the even POVM), Eq. (27) guarantees that the estimator approaches the true value with high probability as the number of measurements N increases. Note that the Bayesian inference may return estimates far from the true value as discussed in [17].

Furthermore, the asymptotic variance of our estimator can achieve the Cramér-Rao lower bound when N is large. To show this result, we first introduce the following total classical/quantum Fisher information of our estimator:

$$\mathcal{I}_{c/q,\text{tot}}(\theta^*) = N \sum_{m=1}^M \mathbf{E}_{\mathbf{X}_{m-1}} [\mathcal{I}_{c/q}(\alpha_m(\mathbf{X}_{m-1}); \theta^*)]. \quad (29)$$

The derivation is provided in Appendix C. Since Theorem 1 states that $\alpha_m(\mathbf{X}_{m-1})$ becomes a constant with high probability as N increases, the total Fisher information also converges as follows;

$$\frac{\mathcal{I}_{c/q,\text{tot}}(\theta^*)}{N} \rightarrow \frac{\mathcal{I}_{c/q,\text{tot}}^*(\theta^*)}{N}, \quad (30)$$

where $\mathcal{I}_{c/q,\text{tot}}^*(\theta^*)$ is the asymptotic value of the total classical/quantum Fisher information defined as

$$\mathcal{I}_{c/q,\text{tot}}^*(\theta^*) := N \sum_{m=1}^M \mathcal{I}_{c/q}(\alpha_m^*; \theta^*). \quad (31)$$

Here, we provide the convergence theorem for the distribution of our estimator.

Theorem 2. (Asymptotic normality; informal version.) *If $\hat{\theta}_M$ is a maximum likelihood estimator of $\mathcal{L}_M(\theta; \mathbf{X}_M)$, then the following convergence holds;*

$$\sqrt{\mathcal{I}_{c,\text{tot}}^*(\arccos \langle \mathcal{O} \rangle)} \left(\cos \hat{\theta}_M - \langle \mathcal{O} \rangle \right) \rightarrow \mathcal{N}(0, 1 - \langle \mathcal{O} \rangle^2), \quad (32)$$

where \mathcal{N} denotes a centered normal distribution with variance $1 - \langle \mathcal{O} \rangle^2$, and \rightarrow means the convergence in distribution as N increases.

This theorem shows that the distribution of our estimator $\cos \hat{\theta}_M$ gets arbitrarily close to the normal distribution with mean $\langle \mathcal{O} \rangle$ in large N . In addition, the asymptotic variance of our estimator is equivalent to the inverse of the asymptotic value of the total classical Fisher information. Thus, our estimator can asymptotically achieve the classical Cramér-Rao lower bound. In the next section, we demonstrate that the asymptotic properties hold in practical N .

Moreover, recalling the optimality of the even POVM (14), the total classical Fisher information is likely sufficiently close to the total quantum Fisher information, as the number of qubits increases;

$$\mathcal{I}_{c,\text{tot}}^*(\theta^*) \approx \mathcal{I}_{q,\text{tot}}^*(\theta^*). \quad (33)$$

Since the optimization in Eq. (26) decreases the approximation error in Eq. (33), it depends on the selection of the set of optimization ranges $\{D_k\}_{k=1}^{M-1}$. In the next section, we demonstrate that the approximation error is sufficiently small for *almost all* θ^* , i.e., the total classical Fisher information of our algorithm can be sufficiently close to its total quantum Fisher information with use of a specific set $\{D_k\}_{k=1}^{M-1}$.

IV. NUMERICAL EXPERIMENT

In this section, we numerically verify the performance of the proposed algorithm. First, in the practical (i.e., a few thousand of) measurement number N , we demonstrate that the asymptotic properties shown in the previous section hold. Next, by evaluating the asymptotic value of the total Fisher information, we confirm that the proposed algorithm retains a large Fisher information regardless of the target value θ^* . We also show that the total classical Fisher information becomes sufficiently close to the quantum Fisher information for a system of dozens of qubits.

A. Asymptotic properties with respect to the number of measurement

To demonstrate the properties of our algorithm, we numerically evaluate the root mean squared error (RMSE)

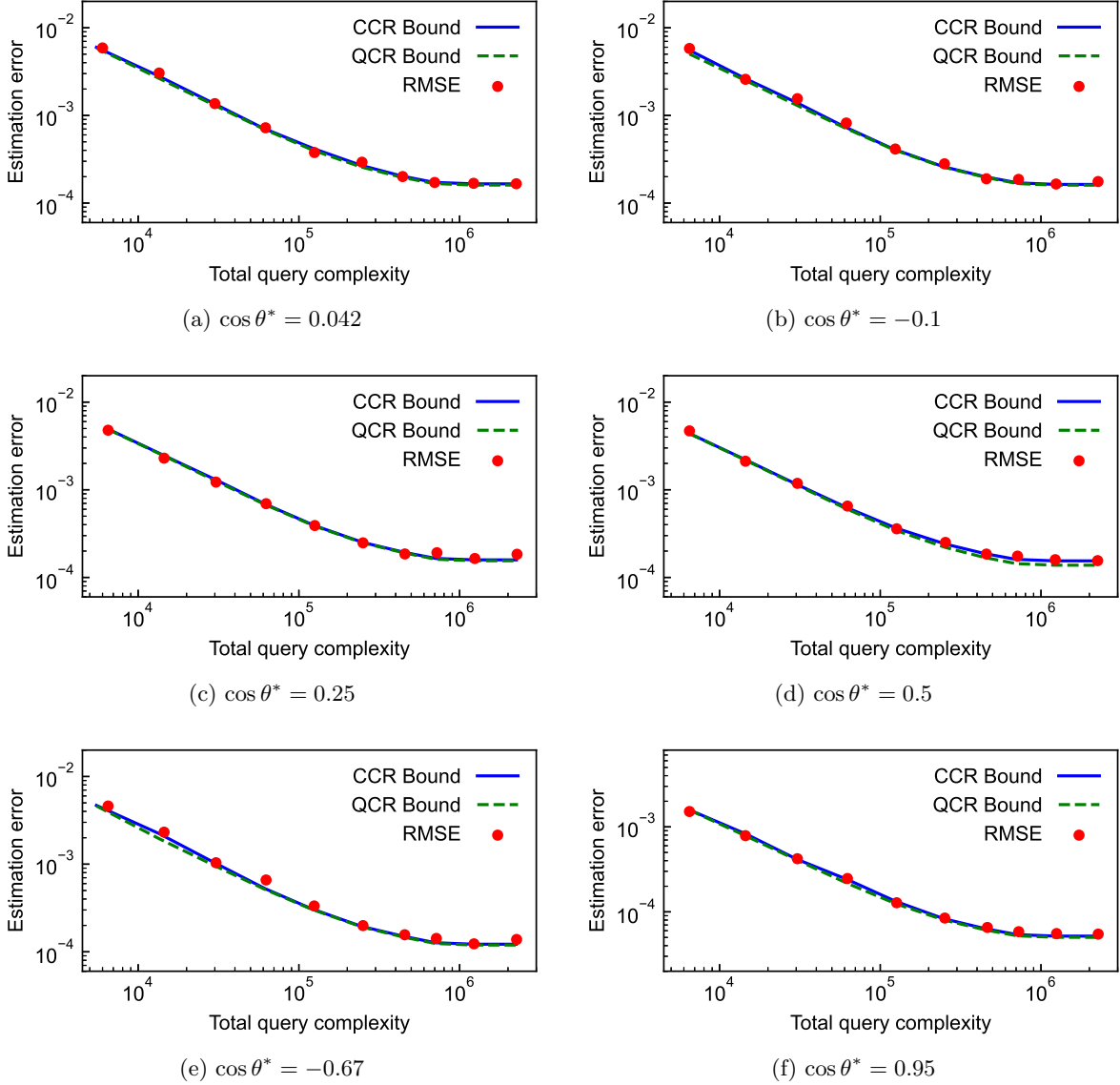


FIG. 2. The estimation error and the total query complexity for several target values. The root mean squared error (RMSE) of the estimator $\cos \hat{\theta}$ is evaluated 200 trials. Since the total number of queries is a random variable in our method, the RMSE was plotted as a function of the maximum value of the realized total number of queries. The blue solid line and green dashed line represent the asymptotic values of CCR/QCR bounds obtained from the corresponding classical/quantum Fisher information $\mathcal{I}_{c/q,tot}^*(\theta^*)$, respectively.

of $\cos \hat{\theta}$ defined as

$$\begin{aligned} \text{RMSE} [\cos \hat{\theta}] &:= \sqrt{\mathbf{E}_{\hat{\theta}} \left[\left(\cos \hat{\theta} - \cos \theta^* \right)^2 \right]} \\ &\simeq \sqrt{\frac{1}{\#} \sum_{i=1}^{\#} \left(\cos \hat{\theta}[i] - \cos \theta^* \right)^2}, \end{aligned} \quad (34)$$

where $\#$ is the total number of trials, and $\hat{\theta}[i]$ denotes the estimate of i th trial. In the following, we use $\# = 200$ samples to evaluate the RMSE. We assume the depolarization noise with the parameters $p_s = 1$ and $p_q = 0.99$.

The number of qubits is set to 20, which corresponds to the system dimension $d = 2^{20}$. We also set the number of measurements as $N = 500$ for each circuit. To obtain the maximum likelihood estimates, we used a modified brute force method, in which the search domain becomes narrowed as the measurement process proceeds. The amplified level α_k of the k th measurement process ($k = 2, \dots, M$) was determined from the maximum likelihood estimate $\hat{\theta}_{k-1}$ and the optimization range D_{k-1} . Here, the discrete set D_{k-1} is set to

$$D_{k-1} := \{2^{k-1}, 2^{k-1} + 1, \dots, 2^k\}. \quad (35)$$

The exponential increase of the number of elements comes from the following fact; the previous research [38] unveiled that, when there is no noise, the exponential increment sequence $m_k = 2^{k-1}$ can achieve the Heisenberg limit in the context of amplitude estimation method reviewed in Section II.

Figure 2 shows the relationship between the total number of queries and the estimation error. Here, the total number of queries is defined by $N \sum_{k=1}^M \alpha_k$, and the red plots correspond to $M = 3, 4, \dots, 12$ from left to right in each panel. Since the total number of queries is a random variable due to the randomness of α_k , we plotted the RMSE as a function of the maximum value of the total number of queries realized in $\# = 200$ trials. In addition, we calculate the classical Cramér-Rao (CCR) lower bound and the quantum Cramér-Rao (QCR) lower bound, using the true value θ^* and the asymptotic sequence $\{\alpha_k^*\}_{k=1}^M$ as in Eq. (31). It is worth noting that the difference between the asymptotic CCR/QCR bounds and the bounds obtained from the $\# = 200$ average of the realized total Fisher information can be negligible. This is because the amplified levels are almost identical to $\{\alpha_k^*\}_{k=1}^M$ as shown in Appendix D. For the six target values, the RMSE nearly achieves the CCR bound, and the ratio of the RMSE to the CCR bound is at most 1.25. Thus, $N = 500$ might be sufficient to obtain the asymptotic property (32) in the current noise condition. In Appendix E, we have confirmed this in a more noisy condition with $p_s = 1$ and $p_q = 0.90$. Note that if we employ larger N such as the maximum number of shots available in real quantum devices, Eq. (32) guarantees that the ratio gets closer to one. On the other hand, as the total number of queries increases, the CCR/QCR bounds become saturated around $M = 10$. This is because the Fisher information in the case $M > 10$ is overwhelmed by the depolarization noise. When the circuit depth is limited as in [32], one effective strategy is to fix the amplified level at the maximum point of the classical Fisher information after $\max D_k$ exceeds this point. Fixing the amplified level based on this strategy, our method turns to be a simple maximum likelihood estimation method, which also satisfies the asymptotic properties in Section III, with the full use of the given noisy quantum device. In addition, it should be emphasized that the CCR bound is nearly identical to the QCR bound. As seen in the next subsection, this holds for almost all θ^* .

B. Efficiency of our estimator

As described in Section III, the classical Fisher information associated with measurements (14) and (19) vanishes at certain points of θ^* . However, our algorithm can avoid those points and retain large Fisher information thanks to the optimization of amplified levels. To confirm this advantage, we calculate the asymptotic total Fisher information $\mathcal{I}_{c/q,tot}^*(\theta^*)$ for every $\theta^* \in (0, \pi)$. In the following, we take the same experimental setting

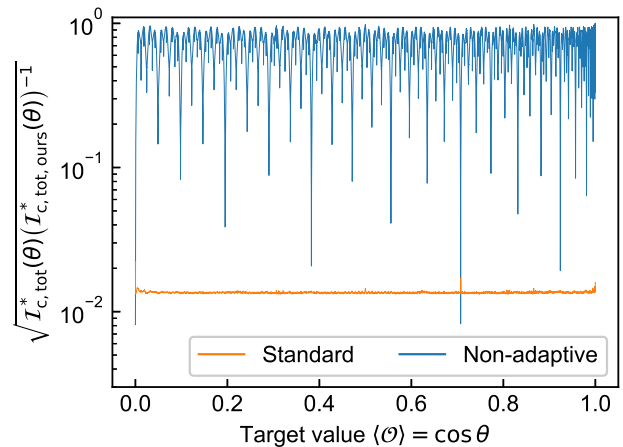


FIG. 3. Comparison of the total classical Fisher information of our method and that of other method. Orange (bottom) and blue (top) lines represent the ratio of the Fisher information corresponding to standard sampling method $\alpha_k^* = 1$ and the non-adaptive method with sequence $\alpha_1^* = 1$, $\alpha_k^* = 2^k$ ($k \geq 2$), respectively. As for our classical Fisher information, we used its asymptotic value to plot this figure.

as that in the previous subsection. The number of measurement processes M is set to nine, which includes the maximum point of the quantum Fisher information under the current noise level.

Figure 3 shows the target value dependency of the ratio between the (asymptotic) total classical Fisher information of our method and that of other methods. The classical Fisher information for the standard sampling method, which is usually employed for VQE [2] calculations, is defined by Eq. (31) with $\alpha_k^* = 1 \forall k$, while that for the non-adaptive method [35, 37, 38] is defined by Eq. (31) with $\alpha_1^* = 1$, $\alpha_k^* = 2^k \forall k \geq 2$. Since the classical Fisher information for the standard sampling is constant regardless of the target value in the current setting, its plot reflects the behavior of our classical Fisher information to the target value. In contrast to our total classical Fisher information, the performance of non-adaptive method heavily depends on the target value. In addition, there are some target values for which the estimation error bound deviates by more than two order of magnitude from ours. Therefore, when the amplified level $\{\alpha_k\}_{k=1}^M$ is chosen non-adaptively, even if the asymptotic properties of maximum likelihood estimators hold, the estimation efficiency is significantly decreased. Comparing to the standard sampling method, we observe improvement of about two order of magnitude for all target values. The improvement depends on the noise level, and therefore the estimation efficiency is further accelerated when there is less noise. Consequently, we confirm that our total classical Fisher information retains large Fisher information regardless of the target value.

Finally, Fig. 4 shows the ratio of the asymptotic total classical and quantum Fisher information. For almost

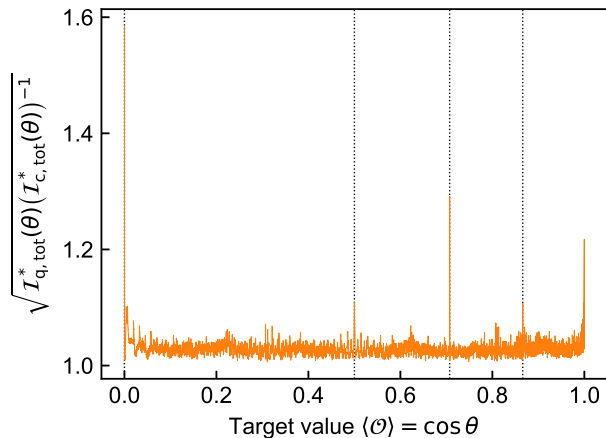


FIG. 4. Comparison of the asymptotic total classical and quantum Fisher information of our method in twenty qubits. The vertical dotted lines represent the target values corresponding to $\theta^* = \pi/j$, $j = 2, 3, 4, 6$ from left to right.

all target values, the difference between asymptotic values of CCR bound and the QCR bound is sufficiently small, which is in line with the results of the previous subsection. In general, the QCR bound, which means the ultimate limit of the estimation precision, can only be achieved when using the optimal measurement tailored for a given quantum state. The results demonstrate that Eq. (33) holds; that is, our estimation method can select the almost optimal measurements (or POVM) with respect to its Fisher information. For the target values $\theta^* = \pi/2, \pi/3, \pi/4, \pi/6$, the difference of the QCR bound and the CCR bound is slightly larger than that for other target values. This is because values of $(m+1)\theta^* \pmod{2\pi}$ obtained from the amplitude amplification are limited at these target values, and therefore the classical Fisher information cannot get close to the quantum Fisher information, i.e., $(m+1)\theta^*$ does not get sufficiently close to $k\pi/2$, $k \in \mathbb{Z}$ (not identical to $k\pi/2$, see Appendix B). Fortunately, the peaks at these points in Fig. 4 are very sharp, and thus they may be ignored in usual. This is because, when the target values shift slightly from these points, the values of $(m+1)\theta^* \pmod{2\pi}$ will fill the domain $[0, 2\pi)$ exponentially in the optimization of amplified levels on the current $\{D_k\}_k$.

V. CONCLUSIONS

We have proposed a quantum-enhanced mean value estimation method in a noisy environment that achieves the ultimate precision characterized by the quantum Fisher information. This method employs a modified maximum likelihood estimation with the adaptive measurements consisting of two-types of POVMs and the amplitude amplifications, which are assumed to introduce a depolarization noise. The POVMs and the number of query of the amplitude amplification operators are optimized in order to enhance the classical Fisher information so that it achieves the quantum Fisher information. Importantly, thanks to the maximum likelihood formulation, we can show that our estimator enjoys some provable statistical properties such as consistency and asymptotic normality.

To show the effectiveness of the proposed estimator, we provided thorough numerical experiments. The asymptotic statistical properties are evaluated in terms of the root mean squared error (RMSE), for several target values; the result was that, in all cases, the RMSE saturates the asymptotic classical and quantum Cramér-Rao lower bound, with not a large number of measurements. In particular, we confirmed that the classical Fisher information almost saturates the ultimate quantum Fisher information in a large system dimension $d = 2^{20}$ (corresponding to a twenty-qubit system). In addition, we studied how the total Fisher information depends on the target value by evaluating the asymptotic classical/quantum Cramér-Rao lower bounds. Although the previous researches [18, 37] imply that the classical Fisher information significantly deteriorates for certain target values under depolarization noise, the proposed estimator retains a large Fisher information regardless of the target value, due to the adaptive optimization.

Acknowledgements: K.W. and K.F. thank IPA for its support through MITOU target program. We would like to thank Dr. Yasunari Suzuki, Dr. Yuuki Tokunaga, and Dr. Tomoki Tanaka for helpful discussions. This work was supported by MEXT Quantum Leap Flagship Program Grant Number JPMXS0118067285 and JPMXS0120319794.

-
- [1] M. Cerezo, A. Arrasmith, R. Babbush, S. C. Benjamin, S. Endo, K. Fujii, J. R. McClean, K. Mitarai, X. Yuan, L. Cincio, *et al.*, Variational quantum algorithms, *Nature Reviews Physics* **3**, 625 (2021).
 - [2] A. Peruzzo, J. McClean, P. Shadbolt, M.-H. Yung, X.-Q. Zhou, P. J. Love, A. Aspuru-Guzik, and J. L. O’Brien, A variational eigenvalue solver on a photonic quantum processor, *Nature communications* **5**, 1 (2014).
 - [3] A. Kandala *et al.*, Hardware-efficient variational quantum

- eigensolver for small molecules and quantum magnets, *Nature* **549**, 242 (2017).
- [4] B. Fuller, C. Hadfield, J. R. Glick, T. Imamichi, T. Itoko, R. J. Thompson, Y. Jiao, M. M. Kagele, A. W. Blom-Schieber, R. Raymond, *et al.*, Approximate solutions of combinatorial problems via quantum relaxations, arXiv preprint arXiv:2111.03167 (2021).
- [5] Q. Gao *et al.*, Applications of quantum computing for investigations of electronic transi-

- tions in phenylsulfonyl-carbazole TADF emitters, *npj Comput. Mater.* **7**, 1 (2021).
- [6] D. Amaro, M. Rosenkranz, N. Fitzpatrick, K. Hirano, and M. Fiorentini, A case study of variational quantum algorithms for a job shop scheduling problem, *EPJ Quantum Technology* **9**, 5 (2022).
- [7] C. Zoufal, R. V. Mishmash, N. Sharma, N. Kumar, A. Sheshadri, A. Deshmukh, N. Ibrahim, J. Gacon, and S. Woerner, Variational quantum algorithm for unconstrained black box binary optimization: Application to feature selection, *arXiv preprint arXiv:2205.03045* (2022).
- [8] Y. Li and S. C. Benjamin, Efficient variational quantum simulator incorporating active error minimization, *Physical Review X* **7**, 021050 (2017).
- [9] Y.-X. Yao, N. Gomes, F. Zhang, C.-Z. Wang, K.-M. Ho, T. Iadecola, and P. P. Orth, Adaptive variational quantum dynamics simulations, *PRX Quantum* **2**, 030307 (2021).
- [10] M. Benedetti, M. Fiorentini, and M. Lubasch, Hardware-efficient variational quantum algorithms for time evolution, *Physical Review Research* **3**, 10.1103/physrevresearch.3.033083 (2021).
- [11] K. Wada, R. Raymond, Y.-y. Ohnishi, E. Kaminishi, M. Sugawara, N. Yamamoto, and H. C. Watanabe, Simulating time evolution with fully optimized single-qubit gates on parametrized quantum circuits, *Physical Review A* **105**, 062421 (2022).
- [12] R. LaRose, A. Tikku, É. O’Neel-Judy, L. Cincio, and P. J. Coles, Variational quantum state diagonalization, *npj Quantum Information* **5**, 1 (2019).
- [13] M. Cerezo, K. Sharma, A. Arrasmith, and P. J. Coles, Variational quantum state eigensolver, *npj Quantum Information* **8**, 1 (2022).
- [14] J. Tilly, H. Chen, S. Cao, D. Picozzi, K. Setia, Y. Li, E. Grant, L. Wossnig, I. Rungger, G. H. Booth, *et al.*, The variational quantum eigensolver: a review of methods and best practices, *Physics Reports* **986**, 1 (2022).
- [15] D. Wecker, M. B. Hastings, and M. Troyer, Progress towards practical quantum variational algorithms, *Physical Review A* **92**, 042303 (2015).
- [16] J. F. Gonthier, M. D. Radin, C. Buda, E. J. Daskocil, C. M. Abuan, and J. Romero, Identifying challenges towards practical quantum advantage through resource estimation: the measurement roadblock in the variational quantum eigensolver, *arXiv preprint arXiv:2012.04001* (2020).
- [17] P. D. Johnson, A. A. Kunitsa, J. F. Gonthier, M. D. Radin, C. Buda, E. J. Daskocil, C. M. Abuan, and J. Romero, Reducing the cost of energy estimation in the variational quantum eigensolver algorithm with robust amplitude estimation, *arXiv preprint arXiv:2203.07275* (2022).
- [18] G. Wang, D. E. Koh, P. D. Johnson, and Y. Cao, Minimizing estimation runtime on noisy quantum computers, *PRX Quantum* **2**, 010346 (2021).
- [19] H. Cramér, *Mathematical methods of statistics.*, (1946).
- [20] J. Shao, *Mathematical statistics* (Springer Science & Business Media, 2003).
- [21] A. S. Holevo, *Probabilistic and statistical aspects of quantum theory*, Vol. 1 (Springer Science & Business Media, 2011).
- [22] M. Hayashi, *Quantum information* (Springer, 2006).
- [23] C. W. Helstrom, Quantum detection and estimation theory, *Journal of Statistical Physics* **1**, 231 (1969).
- [24] C. Helstrom, The minimum variance of estimates in quantum signal detection, *IEEE Transactions on information theory* **14**, 234 (1968).
- [25] S. L. Braunstein and C. M. Caves, Statistical distance and the geometry of quantum states, *Physical Review Letters* **72**, 3439 (1994).
- [26] M. G. Paris, Quantum estimation for quantum technology, *International Journal of Quantum Information* **7**, 125 (2009).
- [27] C. L. Degen, F. Reinhard, and P. Cappellaro, Quantum sensing, *Reviews of modern physics* **89**, 035002 (2017).
- [28] P. Faist, M. P. Woods, V. V. Albert, J. M. Renes, J. Eisert, and J. Preskill, Time-energy uncertainty relation for noisy quantum metrology, in *Quantum Information and Measurement* (Optical Society of America, 2021) pp. W2A–3.
- [29] S. Aaronson and P. Rall, Quantum approximate counting, simplified, in *Symposium on Simplicity in Algorithms* (SIAM, 2020) pp. 24–32.
- [30] D. Grinko, J. Gacon, C. Zoufal, and S. Woerner, Iterative quantum amplitude estimation, *npj Quantum Information* **7**, 1 (2021).
- [31] K. Nakaji, Faster amplitude estimation, *arXiv preprint arXiv:2003.02417* (2020).
- [32] A. Callison and D. Browne, Improved maximum-likelihood quantum amplitude estimation, *arXiv preprint arXiv:2209.03321* (2022).
- [33] E. G. Brown, O. Goktas, and W. Tham, Quantum amplitude estimation in the presence of noise, *arXiv preprint arXiv:2006.14145* (2020).
- [34] T. Giurgica-Tiron, I. Kerenidis, F. Labib, A. Prakash, and W. Zeng, Low depth algorithms for quantum amplitude estimation, *Quantum* **6**, 745 (2022).
- [35] S. Uno, Y. Suzuki, K. Hisanaga, R. Raymond, T. Tanaka, T. Onodera, and N. Yamamoto, Modified grover operator for quantum amplitude estimation, *New Journal of Physics* **23**, 083031 (2021).
- [36] J. M. Martyn, Z. M. Rossi, A. K. Tan, and I. L. Chuang, Grand unification of quantum algorithms, *PRX Quantum* **2**, 040203 (2021).
- [37] T. Tanaka, Y. Suzuki, S. Uno, R. Raymond, T. Onodera, and N. Yamamoto, Amplitude estimation via maximum likelihood on noisy quantum computer, *Quantum Information Processing* **20**, 1 (2021).
- [38] Y. Suzuki, S. Uno, R. Raymond, T. Tanaka, T. Onodera, and N. Yamamoto, Amplitude estimation without phase estimation, *Quantum Information Processing* **19**, 1 (2020).
- [39] T. Tanaka, S. Uno, T. Onodera, N. Yamamoto, and Y. Suzuki, Noisy quantum amplitude estimation without noise estimation, *Physical Review A* **105**, 012411 (2022).
- [40] G. Brassard, P. Hoyer, M. Mosca, and A. Tapp, Quantum amplitude amplification and estimation, *Contemporary Mathematics* **305**, 53 (2002).
- [41] D. E. Koh, G. Wang, P. D. Johnson, and Y. Cao, A framework for engineering quantum likelihood functions for expectation estimation, *arXiv preprint arXiv:2006.09349* (2020).
- [42] Z. Jiang, Quantum fisher information for states in exponential form, *Physical Review A* **89**, 032128 (2014).
- [43] Y. Yao, L. Ge, X. Xiao, X. Wang, and C. Sun, Multiple phase estimation for arbitrary pure states under white

noise, Physical Review A **90**, 062113 (2014).

VI. APPENDIX

A. Fisher information and Cramér-Rao inequality

Let \mathbf{X} be a multi-dimensional discrete random variable following a joint probability distribution $\mathcal{L}(\mathbf{x}; \theta)$, where θ is a parameter in \mathbb{R} (in our case, the domain is $(0, \pi)$). We try to estimate $g(\theta)$, where $g(\cdot)$ is a bijective function, by constructing an estimator $\hat{e}(\mathbf{X})$ for $g(\theta)$. In general, if $\hat{e}(\mathbf{X})$ is an unbiased estimator, i.e., $\mathbf{E}_{\mathbf{X}}[\hat{e}(\mathbf{X})] = g(\theta)$, then the mean squared error of $\hat{e}(\mathbf{X})$ is bounded by so-called Cramér-Rao inequality [20]

$$\text{MSE}[\hat{e}(\mathbf{X})] \geq \left(\frac{\partial g(\theta)}{\partial \theta} \right)^2 \mathcal{I}_{\text{c,tot}}^{-1}(\theta), \quad (\text{A.1})$$

where $\mathcal{I}_{\text{c,tot}}(\theta)$ is the total classical Fisher information defined as

$$\mathcal{I}_{\text{c,tot}}(\theta) := \mathbf{E}_{\mathbf{X}} \left[\left\{ \frac{\partial}{\partial \theta} \ln \mathcal{L}(\theta; \mathbf{X}) \right\}^2 \right]. \quad (\text{A.2})$$

For simplicity, we write $\partial/\partial\theta$ as ∂_{θ} in the below.

Consider the estimation problem for a single parameter embedded in a quantum state $\rho(\theta)$. Fixing a POVM for measuring the quantum state, we can obtain the probability distribution parameterized by θ similar as described above. However, there exists a degree of freedom for the selection of a POVM in quantum case. Utilizing the degree of freedom, the lower bound of Eq. (A.1) can in fact be improved.

This result is known as the following quantum Cramér-Rao inequality [22–26]

$$\mathcal{I}_{\text{q}}(\theta) \geq \mathcal{I}_{\text{c}}(\theta), \quad (\text{A.3})$$

where \mathcal{I}_{c} is the classical Fisher information associated with the probability distribution for a POVM $\{M_k\}_k$ and the target state $\rho(\theta)$. Here, \mathcal{I}_{q} denotes the quantum Fisher information defined by only the target state $\rho(\theta)$ as follows,

$$\mathcal{I}_{\text{q}}(\theta) := \text{tr} [L_{\text{SLD}}^2 \rho(\theta)], \quad (\text{A.4})$$

where L_{SLD} is the symmetric logarithmic derivative (SLD), which is defined as the Hermitian operator satisfying $2\partial_{\theta}\rho(\theta) = L_{\text{SLD}}\rho(\theta) + \rho(\theta)L_{\text{SLD}}$. Note that the inequality Eq. (A.3) holds for any POVM $\{M_k\}_k$ independent to θ . Accordingly, the quantum Fisher information characterizes the limitation of estimation precision which cannot overcome with any measurements.

B. Analysis for several POVMs

In our algorithm, we aim to estimate the target parameter $\theta \in (0, \pi)$ embedded into the quantum state

$$\rho_{\mathcal{D}}(m; \theta) = p_s p_q^m \rho(m; \theta) + \frac{1 - p_s p_q^m}{d} I_n. \quad (\text{B.1})$$

Let us consider the additional quantum operation \mathcal{O} into Eq. (B.1) and the following measurement

$$M_0 := |\bar{0}\rangle \langle \bar{0}|, \quad M_1 := |\bar{1}\rangle \langle \bar{1}|, \quad M_2 := I_n - M_0 - M_1. \quad (\text{B.2})$$

Here, the additional operation \mathcal{O} simply turns the frequency of trigonometric functions in $\rho(m; \theta)$ into $2(m+1)$, which is appropriate to the total number of querying A or A^\dagger . Note that the POVM has insightful meanings. M_0 and M_1 correspond to the measurement in the subspace basis $|\bar{0}\rangle$ and $|\bar{1}\rangle$. Here, $|\bar{1}\rangle$ implicitly depends on the true value. M_2 tells us that the measured state is not in the subspace \mathcal{S} .

From the direct calculation, we can confirm that for certain θ the classical Fisher information $\mathcal{I}'_{\text{c}}(\theta)$ for the probability distribution

$$\{\text{tr}[M_k \mathcal{O} \rho_{\mathcal{D}}(m; \theta) \mathcal{O}]\}_{k=0}^2, \quad (\text{B.3})$$

is equal to the quantum Fisher information as follows

$$\begin{aligned} \mathcal{I}'_{\text{c}}(\theta) &= 4(\eta')^2 \sin^2 [2(m+1)\theta] (m+1)^2 \\ &\times \left\{ \eta' + \frac{2(1-\eta')}{d} - \frac{d(\eta')^2 \cos^2 [2(m+1)\theta]}{d\eta' + 2(1-\eta')} \right\}^{-1} \\ &\leq \frac{4d(\eta')^2 (m+1)^2}{d\eta' + 2(1-\eta')}, \end{aligned} \quad (\text{B.4})$$

where $\eta' := p_s p_q^{m+1/2}$ and the condition for the equality is $\sin [2(m+1)\theta] = \pm 1$. The r.h.s. in the final line in fact corresponds to the quantum Fisher information for the state $\rho_{\mathcal{D}}(m; \theta)$ with \mathcal{O} . Thus, for θ satisfying the equality condition, the POVM Eq. (B.2) is optimal in its classical Fisher information for the quantum Cramér-Rao inequality. Note that the eigenstates of SLD operator are known as an optimal measurement that can achieve quantum Fisher information exactly [25]. Actually, this measurement can be constructed as M'_0, M'_1 , and M_2 , where one-dimensional projectors M'_0 and M'_1 are obtained from a linear combination of $|\bar{0}\rangle$ and $|\bar{1}\rangle$ with coefficients depending on the true target value.

Although the POVM Eq. (B.2) is an optimal measurement for certain θ , it is difficult to implement the measurement especially for M_1 , which depends on θ . Therefore, in this paper we focus on the 2-valued POVM in Eq. (14). This POVM removes θ -dependency in Eq. (B.2) at cost of exact achievability for the quantum Fisher information. To compare the classical Fisher information associated with the 2-valued POVM with the quantum

Fisher information, we first clarify the behavior of the classical Fisher information $\mathcal{I}_c^{(\text{even})}(m; \theta)$:

$$\begin{aligned} & \lim_{d \rightarrow \infty} \mathcal{I}_c^{(\text{even})}(m; \theta) \\ &= \begin{cases} 0, & \cos[(m+1)\theta] = 0 \\ \frac{4\eta'(m+1)^2 \sin^2[(m+1)\theta]}{1 - \eta' \cos^2[(m+1)\theta]}, & \cos[(m+1)\theta] \neq 0 \end{cases}. \end{aligned} \quad (\text{B.5})$$

Note that for $\cos[(m+1)\theta] \neq 0$, we obtain

$$\begin{aligned} \lim_{d \rightarrow \infty} \mathcal{I}_c^{(\text{even})}(m; \theta) &= \frac{4\eta'(m+1)^2 \sin^2[(m+1)\theta]}{1 - \eta' \cos^2[(m+1)\theta]} \\ &\leq 4\eta'(m+1)^2 \\ &= \lim_{d \rightarrow \infty} \mathcal{I}_q^{(\text{even})}(m), \end{aligned} \quad (\text{B.6})$$

where we rewrite the quantum Fisher information for the state $\rho_{\mathcal{D}}(m; \theta)$ with \mathcal{O} as

$$\mathcal{I}_q^{(\text{even})}(m) = \frac{4d(\eta')^2(m+1)^2}{d\eta' + 2(1 - \eta')}. \quad (\text{B.7})$$

The inequality of the second line in Eq. (B.6) holds for $\cos[(m+1)\theta] = 0$ even though $\mathcal{I}_c^{(\text{even})}(m; \theta)$ vanishes at the point as shown in Eq. (B.5). Therefore, the classical Fisher information is not continuous at $\cos[(m+1)\theta] = 0$ in the limit $d = 2^n \rightarrow \infty$, and approaching this singular point, the deviation between the classical Fisher information and quantum Fisher information become arbitrarily small. Importantly, the classical Fisher information for the 2-valued POVM Eq. (14) can be sufficiently close to the quantum Fisher information under the certain condition. Note that since this discontinuity makes the opti-

mization problem in Eq. (26) unstable around the singular points, we introduce the regularization term into the objective function.

As for the other 2-valued POVM Eq. (19), the quantum Fisher information should be calculated for the quantum state Eq. (B.1) with the additional operation \mathcal{O} since the POVM is dependent to \mathcal{O} . Comparing the Fisher information $\mathcal{I}_{q/c}(\alpha; \theta)$ for $\alpha = 2m+1$, we can obtain the following inequality for $d > 2$

$$\begin{aligned} \mathcal{I}_c^{(\text{odd})}(m; \theta) &= \frac{(2m+1)^2 (p_s p_q^m)^2 \sin^2[(2m+1)\theta]}{4\mathbf{P}_{\mathcal{D}}^{(\text{odd})}(m; \theta) \left(1 - \mathbf{P}_{\mathcal{D}}^{(\text{odd})}(m; \theta)\right)} \\ &= \frac{(2m+1)^2 (p_s p_q^m)^2 \sin^2[(2m+1)\theta]}{1 - (p_s p_q^m)^2 \cos^2[(2m+1)\theta]} \\ &\leq (2m+1)^2 (p_s p_q^m)^2 \\ &< \mathcal{I}_q^{(\text{odd})}(m). \end{aligned} \quad (\text{B.8})$$

It is worth noting that unlike the even classical Fisher information, the odd classical Fisher information deviates from the quantum Fisher information even if the number of qubits increases.

C. Statistical structure of our algorithm

In our model, the distribution of random variables \mathbf{X}_M has a hierarchical model such that

$$\mathcal{L}_M(\mathbf{x}_M; \theta) = \prod_{m=1}^M F_m(x^{(m)}; \alpha_m(\mathbf{x}_{m-1}), \theta), \quad (\text{C.1})$$

where F_m is the probability function of Binomial distribution with success probability $\mathbf{P}_{\mathcal{D}}(\alpha_m(\mathbf{x}_{m-1}); \theta)$ and number of trials N_m . Substituting Eq. (C.1) into Eq. (A.2), we obtain the total classical Fisher information as

$$\begin{aligned} \mathcal{I}_{c, \text{tot}}(\theta) &= - \sum_{m=1}^M \mathbf{E}_{\mathbf{X}_m} \left[\partial_{\theta}^2 \ln F_m \left(X^{(m)}; \alpha_m(\mathbf{X}_{m-1}), \theta \right) \right] \\ &= - \sum_{m=1}^M \sum_{\mathbf{x}_m = (x^{(1)}, \dots, x^{(m)})} \partial_{\theta}^2 \ln F_m \left(x^{(m)}; \alpha_m(\mathbf{x}_{m-1}), \theta \right) \mathcal{L}_m(\mathbf{x}_m; \theta) \\ &= - \sum_{m=1}^M \sum_{\mathbf{x}_{m-1} = (x^{(1)}, \dots, x^{(m-1)})} \sum_{x^{(m)}} \partial_{\theta}^2 \ln F_m \left(x^{(m)}; \alpha_m(\mathbf{x}_{m-1}), \theta \right) F_m \left(x^{(m)}; \alpha_m(\mathbf{x}_{m-1}), \theta \right) \mathcal{L}_{m-1}(\mathbf{x}_{m-1}; \theta) \\ &= - \sum_{m=1}^M \sum_{\mathbf{x}_{m-1}} \mathcal{L}_{m-1}(\mathbf{x}_{m-1}; \theta) \sum_{x^{(m)}} \partial_{\theta}^2 \ln F_m \left(x^{(m)}; \alpha_m(\mathbf{x}_{m-1}), \theta \right) F_m \left(x^{(m)}; \alpha_m(\mathbf{x}_{m-1}), \theta \right) \\ &= - \sum_{m=1}^M \sum_{\mathbf{x}_{m-1}} \mathcal{L}_{m-1}(\mathbf{x}_{m-1}; \theta) \mathbf{E}_{Y^{(m)}} \left[\partial_{\theta}^2 \ln F_m \left(Y^{(m)}; \alpha_m(\mathbf{x}_{m-1}), \theta \right) \right], \end{aligned} \quad (\text{C.2})$$

where we used the conditional probability of Eq. (C.1) to the third line. $Y^{(m)}$ denotes a random variable fol-

lowing $F_m(y^{(m)}; \alpha_m(\mathbf{x}_{m-1}), \theta)$, $y^{(m)} \in \{0, 1, \dots, N_m\}$,

where \mathbf{x}_{m-1} is not a random variable. The expectation in the final line corresponds to the classical Fisher information in Eq. (22) multiplied by N_m . Thus, we can write the total classical Fisher information as

$$\mathcal{I}_{c/q,\text{tot}}(\theta) = \sum_{m=1}^M N_m \mathbf{E}_{\mathbf{X}_{m-1}} [\mathcal{I}_{c/q}(\alpha_m(\mathbf{X}_{m-1}); \theta)], \quad (\text{C.3})$$

where we also define the corresponding total quantum Fisher information as $\mathcal{I}_{q,\text{tot}}(\theta)$.

As proved in the following subsection, $\alpha_m(\mathbf{X}_{m-1}) = \alpha_m^*$ holds with high probability for all m as N_m increases, where α_m^* is a solution of the following optimization problem for the target value θ (NOT an estimate $\hat{\theta}$)

$$\alpha_m^* := \underset{\alpha \in D_{m-1}}{\text{argmax}} \mathcal{I}_c(\alpha; \theta) |\sin(\alpha\theta)|^\delta, \quad (\text{C.4})$$

where we define $\alpha_1^* = 1$. Using this, the asymptotic values of the total classical/quantum Fisher information are given by

$$\mathcal{I}_{c/q,\text{tot}}^*(\theta) := \sum_{m=1}^M N_m \mathcal{I}_{c/q}(\alpha_m^*; \theta), \quad (\text{C.5})$$

where it satisfies for $N_m = N \forall m$,

$$\lim_{N \rightarrow \infty} \frac{\mathcal{I}_{c/q,\text{tot}}(\theta)}{N} = \sum_{m=1}^M \mathcal{I}_{c/q}(\alpha_m^*; \theta) = \frac{\mathcal{I}_{c/q,\text{tot}}^*(\theta)}{N}. \quad (\text{C.6})$$

This quantity characterizes the variance of our estimator in asymptotic regime.

D. Proof for statistical properties

Let $\theta^* \in (0, \pi)$ satisfying $\cos \theta^* = \langle \mathcal{O} \rangle$ be a target value to be estimated. Since the objective function in Eq. (C.4) vanishes at $\alpha\theta^* = l\pi$ ($l \in \mathbb{Z}$), then the definition of α_m^* leads to $\alpha_m^* \theta^* \neq l\pi$ for $m = 2, 3, \dots, M$. Thus, we can take an integer z_m satisfying

$$\theta^* \in \Theta^{(m)} := \left(\frac{z_m}{\alpha_m^*} \pi, \frac{z_m + 1}{\alpha_m^*} \pi \right), \quad \forall m, \quad (\text{D.1})$$

and define $\Theta_M := \cap_{m=1}^M \Theta^{(m)}$.

Theorem 1. *There exists a unique maximum likelihood estimator $\hat{\theta}_M$ of $\mathcal{L}_M(\theta; \mathbf{X}_M)$ such that $\cos \hat{\theta}_M \rightarrow \cos \theta^*$ (convergence in probability) with the probability approaching 1 as $N \rightarrow \infty$, and*

$$\lim_{N \rightarrow \infty} P[\alpha_k(\mathbf{X}_{k-1}) = \alpha_k^*] = 1 \quad (\text{D.2})$$

holds for all $k = 2, \dots, M$.

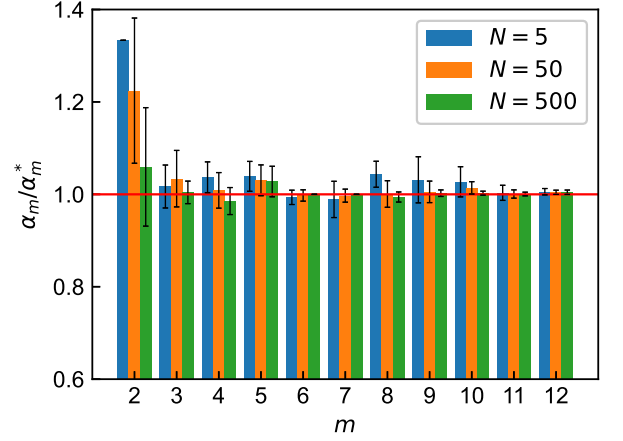


FIG. 5. Convergence of the amplified levels. Here, we employed the target value $\langle \mathcal{O} \rangle = 0.042$. The bar graph represents the average of the realized amplified levels normalized by its asymptotic values over 100 trials, and the error bar denotes the standard deviation.

As a demonstration of Theorem 1, we provide an example of the realized amplified levels in Fig. 5. Here, the experimental settings are equivalent to those in Section IV A. Figure 5 shows that the amplified levels converge rapidly to the asymptotic values, and therefore the total Fisher information and query complexity also show rapid convergence.

Proof. Let $E(m)$ be the following event: $\alpha_k(\mathbf{X}_{k-1}) = \alpha_k^*$ holds for all $k = 1, 2, \dots, m$, and there exists a unique maximum likelihood estimator $\hat{\theta}_m$ of $\mathcal{L}_m(\theta; \mathbf{X}_m)$ which converges to θ^* . Note that if we establish $\hat{\theta}_m \rightarrow \theta^*$, then this immediately leads to $\cos \hat{\theta}_m \rightarrow \cos \theta^*$ due to the continuous mapping theorem.

In the case of $m = 1$, the likelihood function $\mathcal{L}_1(\theta; \mathbf{X}_1)$ is equivalent to $F_1(X^{(1)}; \alpha_1^*, \theta)$. Because the success probability $\mathbf{P}_{\mathcal{D}}(\alpha_1^*; \cdot) : (0, \pi) \rightarrow (0, 1)$ is injective; and the likelihood equation: $\partial_\theta \ln F_1(X^{(1)}; \alpha_1^*, \theta) = 0$ has a unique solution when a solution exists, it follows that

$$P[E(1)] \rightarrow 1 \text{ as } N \rightarrow \infty, \quad (\text{D.3})$$

from the theory of maximum likelihood estimation [20].

Here, we assume that $P[E(M-1)] \rightarrow 1$ for $M \geq 2$. Fixing α in the classical Fisher information $\mathcal{I}_c(\alpha; \theta)$, which includes the regularization $|\sin(\alpha\theta)|^\delta$ in this section, we can confirm that $\mathcal{I}_c(\alpha; \hat{\theta}_{M-1})$ converges smoothly to $\mathcal{I}_c(\alpha; \theta^*)$. If there is a unique point maximizing $\mathcal{I}_c(\alpha; \theta^*)$ in the range of D_{M-1} , then there exists some small number $\epsilon' > 0$, and the following implication holds

$$\left\{ \left| \hat{\theta}_{M-1} - \theta^* \right| < \epsilon' \right\} \subseteq \left\{ \alpha_M(\mathbf{X}_{M-1}) = \alpha_M^* \right\}, \quad (\text{D.4})$$

where $\{\cdot\}$ denotes a set of events such as

$$\left\{ \mathbf{x}_{M-1} : \left| \hat{\theta}_{M-1}(\mathbf{x}_{M-1}) - \theta^* \right| < \epsilon' \right\}. \quad (\text{D.5})$$

Note that even if the maximum point of $\mathcal{I}_c(\alpha; \theta^*)$ in D_{M-1} is not unique, Eq. (D.4) also holds when we adopt the minimum value in a subset \bar{D}_{M-1} of D_{M-1} as the realization of $\alpha_M(\mathbf{X}_{M-1})$. Here, the subset \bar{D}_{M-1} consists of elements in D_{M-1} satisfying

$$\left| \mathcal{I}_c(\alpha; \hat{\theta}_{M-1}) - \mathcal{I}_{c, M-1}^{(\max)}(\hat{\theta}_{M-1}) \right| < \epsilon_{\text{threshold}}, \quad (\text{D.6})$$

where $\epsilon_{\text{threshold}}$ is a small positive number, and

$$\mathcal{I}_{c, M-1}^{(\max)}(\hat{\theta}_{M-1}) := \max_{\alpha \in D_{M-1}} \mathcal{I}_c(\alpha; \hat{\theta}_{M-1}). \quad (\text{D.7})$$

Note that α_M^* is defined as the minimum value of \bar{D}_{M-1} for θ^* . In the limit of $\hat{\theta}_{M-1} \rightarrow \theta^*$, \bar{D}_{M-1} for $\hat{\theta}_{M-1}$ has the same elements in \bar{D}_{M-1} for θ^* , and therefore the implication in Eq. (D.4) holds. From the assumption: $P[E(M-1)] \rightarrow 1$, there exists $N_1^* \in \mathbb{N}$ for all $\eta > 0$ such that

$$P \left[E(M-1) \cap \left\{ \left| \hat{\theta}_{M-1} - \theta^* \right| < \epsilon' \right\} \right] > 1 - \eta \quad (\text{D.8})$$

holds for all $N > N_1^*$. The implication in Eq. (D.4) yields the following inequality

$$\begin{aligned} 1 - \eta &< P \left[E(M-1) \cap \left\{ \left| \hat{\theta}_{M-1} - \theta^* \right| < \epsilon' \right\} \right] \\ &\leq P \left[E(M-1) \cap \left\{ \alpha_M(\mathbf{X}_{M-1}) = \alpha_M^* \right\} \right] \\ &\leq P \left[\left\{ \alpha_k(\mathbf{X}_{k-1}) = \alpha_k^* \forall k \right\} \right]. \end{aligned} \quad (\text{D.9})$$

Note that if $\alpha_k(\mathbf{x}_{k-1}) = \alpha_k^*$ holds for all $k = 1, 2, \dots, M$, then the likelihood function $\mathcal{L}_M(\theta; \mathbf{x}_M)$ can be written as

$$\begin{aligned} \mathcal{L}_M(\theta; \mathbf{x}_M) &= \prod_{m=1}^M F_m \left(x^{(m)}; \alpha_m(\mathbf{x}_{m-1}), \theta \right) \\ &= \prod_{m=1}^M F_m \left(x^{(m)}; \alpha_m^*, \theta \right). \end{aligned} \quad (\text{D.10})$$

On the other hand, Lemma 2 guarantees the existence of some natural number N_2^* such that

$$P[\mathbf{A}] > 1 - \eta, \quad (\text{D.11})$$

for all $N > N_2^*$, where an event \mathbf{A} is defined as

\mathbf{A} : $\prod_{m=1}^M F_m(X^{(m)}; \alpha_m^*, \theta)$ has a unique maximum point $\hat{\theta}_M$ such that $\hat{\theta}_M \rightarrow \theta^*$.

From Eqs. (D.9), (D.11), if we choose $N > \max\{N_1^*, N_2^*\}$, then

$$\begin{aligned} &P[E(M)] \\ &= P \left[\left\{ \mathcal{L}_M(\theta; \mathbf{X}_M) \text{ has a unique maximum point } \hat{\theta}_M \text{ such that } \hat{\theta}_M \rightarrow \theta^* \right\} \cap \left\{ \alpha_k(\mathbf{X}_{k-1}) = \alpha_k^* \forall k = 1, 2, \dots, M \right\} \right] \\ &= P \left[\left\{ \prod_{m=1}^M F_m \left(X^{(m)}; \alpha_m^*, \theta \right) \text{ has a unique maximum point } \hat{\theta}_M \text{ such that } \hat{\theta}_M \rightarrow \theta^* \right\} \cap \left\{ \alpha_k(\mathbf{X}_{k-1}) = \alpha_k^* \forall k \right\} \right] \\ &= P \left[\mathbf{A} \cap \left\{ \alpha_k(\mathbf{X}_{k-1}) = \alpha_k^* \forall k \right\} \right] > 1 - 2\eta. \end{aligned} \quad (\text{D.12})$$

In conclusion, we have proved that $P[E(M)] \rightarrow 1$ also holds, and the mathematical induction establishes the theorem. \square

To prove Lemma 2 or Eq. (D.11), we first establish the existence of a solution for the likelihood equation on F_m .

Lemma 1. *A natural number $m \geq 2$ is fixed arbitrarily. Suppose $P[\alpha_m(\mathbf{X}_{m-1}) = \alpha_m^*] \rightarrow 1$ as the number of*

measurements N increases, then $F_m(X^{(m)}; \alpha_m^, \theta)$ has a unique maximum point $\hat{\theta}^{(m)}$ in Θ_m such that $\hat{\theta}^{(m)} \rightarrow \theta^*$ with the probability approaching 1.*

Proof. We first show

$$P \left[F_m \left(X^{(m)}; \alpha_m^*, \theta^* \right) > F_m \left(X^{(m)}; \alpha_m^*, \theta \right) \right] \rightarrow 1 \quad (\text{D.13})$$

holds for any $\theta \in \Theta_m$, $\theta \neq \theta^*$. The l.h.s can be transformed as

$$\begin{aligned}
& P \left[F_m \left(X^{(m)}; \alpha_m^*, \theta^* \right) > F_m \left(X^{(m)}; \alpha_m^*, \theta \right) \right] \\
&= \sum_{x^{(m)}} \sum_{\mathbf{x}_{m-1}} \mathcal{L}_{m-1} \left(\mathbf{x}_{m-1}; \theta^* \right) F_m \left(x^{(m)}; \alpha_m \left(\mathbf{x}_{m-1} \right), \theta^* \right) \mathbf{1} \left\{ F_m \left(X^{(m)}; \alpha_m^*, \theta^* \right) > F_m \left(X^{(m)}; \alpha_m^*, \theta \right) \right\} \left(x^{(m)} \right) \\
&= \sum_{\alpha'_m \in D_{m-1}} \sum_{\substack{\mathbf{x}_{m-1}: \\ \alpha_m \left(\mathbf{x}_{m-1} \right) = \alpha'_m}} \mathcal{L}_{m-1} \left(\mathbf{x}_{m-1}; \theta^* \right) \sum_{x^{(m)}} F_m \left(x^{(m)}; \alpha'_m, \theta^* \right) \mathbf{1} \left\{ F_m \left(X^{(m)}; \alpha_m^*, \theta^* \right) > F_m \left(X^{(m)}; \alpha_m^*, \theta \right) \right\} \left(x^{(m)} \right) \\
&= \sum_{\alpha'_m \in D_{m-1}} P \left[\alpha_m \left(\mathbf{X}_{m-1} \right) = \alpha'_m \right] \sum_{x^{(m)}} F_m \left(x^{(m)}; \alpha'_m, \theta^* \right) \mathbf{1} \left\{ F_m \left(X^{(m)}; \alpha_m^*, \theta^* \right) > F_m \left(X^{(m)}; \alpha_m^*, \theta \right) \right\} \left(x^{(m)} \right), \quad (\text{D.14})
\end{aligned}$$

where $\mathbf{1}\{\cdot\}(x)$ denotes an indicator function. By assumption, the summation for α'_m of the last line vanishes except for the term with $\alpha'_m = \alpha_m^*$ as N increases. Thus, the remaining term can be written as

$$P \left[F_m \left(Y^{(m)}; \alpha_m^*, \theta^* \right) > F_m \left(Y^{(m)}; \alpha_m^*, \theta \right) \right], \quad (\text{D.15})$$

where $Y^{(m)}$ denotes a random variable following

$$\text{Bin} \left(N, \mathbf{P}_{\mathcal{D}} \left(\alpha_m^*; \theta^* \right) \right). \quad (\text{D.16})$$

Since the probability $\mathbf{P}_{\mathcal{D}} \left(\alpha_m^*; \theta \right)$ is an injective function with respect to $\theta \in \Theta_m$; and its support is independent to θ , these conditions yields

$$P \left[F_m \left(Y^{(m)}; \alpha_m^*, \theta^* \right) > F_m \left(Y^{(m)}; \alpha_m^*, \theta \right) \right] \rightarrow 1, \quad (\text{D.17})$$

as $N \rightarrow \infty$. We can prove this from law of large numbers for independent Bernoulli trials on $Y^{(m)}$ and the non-negativity of the Kullback-Leibler divergence. Combining Eqs. (D.17), (D.14), we complete the proof of Eq. (D.13).

By definition of Θ_m , we can choose a small positive number δ such that $(\theta^* - \delta, \theta^* + \delta) \subset \Theta_m$. Let \mathbf{B}_{\pm} be the following events

$$\mathbf{B}_{\pm}: F_m \left(X^{(m)}; \alpha_m^*, \theta^* \right) > F_m \left(X^{(m)}; \alpha_m^*, \theta^* \pm \delta \right) \text{ holds.}$$

Considering $x^{(m)} \in \mathbf{B}_+ \cap \mathbf{B}_-$, the equation

$$\frac{\partial}{\partial \theta} F_m \left(x^{(m)}; \alpha_m^*, \theta \right) = 0, \quad (\text{D.18})$$

has solutions, and we write $\hat{\theta}^{(m)}$ as the solution closest to θ^* among them. Since the difference between $\hat{\theta}^{(m)}$ and θ^* is less than δ ; and for all $\epsilon > 0$ there exists $N^* \in \mathbb{N}$ such that $P \left[\mathbf{B}_{\pm} \right] > 1 - \epsilon$ for all $N > N^*$ by Eq. (D.13),

we obtain

$$P \left[\left| \hat{\theta}^{(m)} - \theta^* \right| < \delta \right] \geq P \left[\mathbf{B}_+ \cap \mathbf{B}_- \right] > 1 - 2\epsilon. \quad (\text{D.19})$$

In addition, the likelihood equation Eq. (D.18) has a unique solution maximizing $F_m(x^{(m)}; \alpha_m^*, \theta)$ in Θ_m if a solution of Eq. (D.18) exists in Θ_m . Therefore, $\hat{\theta}^{(m)}$ is a unique maximum point of $F_m(x^{(m)}; \alpha_m^*, \theta)$ in Θ_m . \square

Applying Lemma 1 to all the functions $\{F_m\}_m$, we establish the existence of a unique maximum point of the product function $\Pi_m F_m$.

Lemma 2. *Suppose $P[\alpha_k(\mathbf{X}_{k-1}) = \alpha_k^*] \rightarrow 1$ for all $k = 2, \dots, M$; and $\hat{\theta}^{(1)} \rightarrow \theta^*$ (convergence in probability), then there exists a unique maximum point $\hat{\theta}_M$ of the product function $\Pi_{m=1}^M F_m(X^{(m)}; \alpha_m^*, \theta)$ in $(0, \pi)$ such that $\hat{\theta}_M \rightarrow \theta^*$ with the probability approaching 1 as $N \rightarrow \infty$.*

Proof. From the assumption and Lemma 1, we can choose $N^* \in \mathbb{N}$ for all $\epsilon > 0$ such that the probability occurring the following event \mathbf{C} is bigger than $1 - \epsilon$ for all $N > N^*$,

\mathbf{C} : For all m , $\hat{\theta}^{(m)}$ exists in Θ_m , where $\hat{\theta}^{(m)}$ denotes a maximum point of $F_m(X^{(m)}; \alpha_m^*, \theta)$.

Let $\hat{\theta}_{\max}$ ($\hat{\theta}_{\min}$) be the maximum (minimum) value of a set $\{\hat{\theta}^{(m)}\}_m$. Since the product function $\Pi_{m=1}^M F_m$ is a continuous function with respect to θ , it has a maximum point $\hat{\theta}_M$ in $[\hat{\theta}_{\min}, \hat{\theta}_{\max}]$. Note that $\hat{\theta}_{\max}$ and $\hat{\theta}_{\min}$ themselves cannot be a maximum point because the gradients at these points does not vanish, i.e.,

$$\frac{\partial}{\partial \theta} \prod_{m=1}^M F_m \left(X^{(m)}; \alpha_m^*, \theta \right) \Big|_{\theta = \hat{\theta}_{\max}, \hat{\theta}_{\min}} \neq 0, \quad (\text{D.20})$$

where the gradient is positive (negative) for $\hat{\theta}_{\min}$ ($\hat{\theta}_{\max}$), respectively. Therefore, we obtain

$$P \left[\text{there exists a maximum point } \hat{\theta}_M \text{ of } \prod_{m=1}^M F_m \left(X^{(m)}; \alpha_m^*, \theta \right) \text{ in } \Theta_M \text{ such that } \hat{\theta}_M \xrightarrow{P} \theta^* \right] \geq P[\mathbf{C}] > 1 - \epsilon, \quad (\text{D.21})$$

where we use the fact that $\hat{\theta}_{\min}, \hat{\theta}_{\max} \rightarrow \theta^*$ yields $\hat{\theta}_M \rightarrow \theta^*$.

Considering the original domain of θ , i.e., $(0, \pi)$, each F_m is a periodic function and generally maximized at multiple points. Here, $\hat{\theta}^{(m)}$ is one of these points. However, many of these peaks are canceled out each other by multiplication in $\prod_m F_m$ except for the peaks in Θ_M . Since F_1 has a unique global maximum point $\hat{\theta}^{(1)}$, and therefore Θ_M is the only region where all functions F_m have a peak simultaneously as N increases. Consequently, the maximum of $\prod_{m=1}^M F_m(X^{(m)}; \alpha_m^*, \theta)$ in Θ_M becomes the global maximum in $(0, \pi)$. \square

Finally, we prove that when N is large the asymptotic variance of our estimator can achieve the classical Cramér-Rao lower bound.

Theorem 2. *If $\hat{\theta}_M$ is a maximum likelihood estimator on $\mathcal{L}_M(\theta; \mathbf{X}_M)$ such that $\hat{\theta}_M \rightarrow \theta^*$ (convergence in probability), then the following convergence holds*

$$\sqrt{\mathcal{I}_{\text{c,tot}}^*(\theta^*)} (\cos \hat{\theta}_M - \cos \theta^*) \rightarrow \mathcal{N}(0, \sin^2 \theta^*), \quad (\text{D.22})$$

where \mathcal{N} denotes a centered normal distribution with variance $\sin^2 \theta^*$, and \rightarrow means the convergence in distribution as N increases.

Figure 6 shows that fixing the error ϵ , our method gets estimates whose error is less than ϵ with large relative frequency as N increases. This demonstrates Theorem 1. Moreover, the relative frequency in $N = 500$ intersects the Cramér-Rao lower bound around 0.68, which corresponds to the probability of 1-sigma region, and thus this is consistent with Theorem 2.

Proof. According to the Taylor's theorem, we can expand $\partial_\theta \ln \mathcal{L}_M(\theta; \mathbf{X}_M)$ around $\theta = \theta^*$ as

$$\begin{aligned} \partial_\theta \ln \mathcal{L}_M(\theta; \mathbf{X}_M) &= \partial_\theta \ln \mathcal{L}_M(\theta^*; \mathbf{X}_M) \\ &\quad + \partial_\theta^2 \ln \mathcal{L}_M(\theta^*; \mathbf{X}_M)(\theta - \theta^*) \\ &\quad + \frac{1}{2} \partial_\theta^3 \ln \mathcal{L}_M(\theta'; \mathbf{X}_M)(\theta - \theta^*)^2, \end{aligned} \quad (\text{D.23})$$

where θ' denotes some real number between θ and θ^* . Since $\hat{\theta}_M$ is a root of the likelihood equation: $\partial_\theta \mathcal{L}_M(\theta; \mathbf{X}_M) = 0$, we obtain

$$\sqrt{\mathcal{I}_{\text{c,tot}}^*(\theta^*)} (\hat{\theta}_M - \theta^*) = \frac{A}{B - C}, \quad (\text{D.24})$$

$$A := (\mathcal{I}_{\text{c,tot}}^*(\theta^*))^{-1/2} \partial_\theta \ln \mathcal{L}_M(\theta^*; \mathbf{X}_M),$$

$$B := -(\mathcal{I}_{\text{c,tot}}^*(\theta^*))^{-1} \partial_\theta^2 \ln \mathcal{L}_M(\theta^*; \mathbf{X}_M),$$

$$C := (2\mathcal{I}_{\text{c,tot}}^*(\theta^*))^{-1} \partial_\theta^3 \ln \mathcal{L}_M(\theta'; \mathbf{X}_M)(\hat{\theta}_M - \theta^*).$$

Here, we show that A converges to the standard normal distribution. To apply Lemma 3, we first calculate the characteristic function of A replacing $\mathbf{X}_M, \alpha_m \rightarrow \mathbf{Y}_M, \alpha_m^*$, where $\mathbf{Y}_M = (Y^{(1)}, \dots, Y^{(M)})$ is a random vector whose elements follows Binomial distribution $\text{Bin}(N, \mathbf{P}_{\mathcal{D}}(\alpha_m^*; \theta^*))$ independently.

$$\begin{aligned} &\mathbf{E} \left[\exp(it A |_{\mathbf{X}_M, \alpha_m \rightarrow \mathbf{Y}_M, \alpha_m^*}) \right], \quad t \in \mathbb{R}, \\ &= \mathbf{E} \left[\exp \left(\frac{it \sum_{m=1}^M \partial_\theta \ln F_m(Y^{(m)}; \alpha_m^*, \theta^*)}{\sqrt{\mathcal{I}_{\text{c,tot}}^*(\theta^*)}} \right) \right], \\ &= \prod_{m=1}^M \left(\mathbf{E} \left[\exp \left(\frac{it \partial_\theta \ln f_m(Y_1^{(m)}; \alpha_m^*, \theta^*)}{\sqrt{\mathcal{I}_{\text{c,tot}}^*(\theta^*)}} \right) \right] \right)^N \\ &= \prod_{m=1}^M \left(1 - \frac{t^2}{2N} \frac{\mathcal{I}_{\text{c}}(\alpha_m^*; \theta^*)}{\sum_{m=1}^M \mathcal{I}_{\text{c}}(\alpha_m^*; \theta^*)} + o\left(\frac{1}{N}\right) \right)^N \\ &\rightarrow \exp \left(-\frac{t^2}{2} \right), \end{aligned} \quad (\text{D.25})$$

where $Y_1^{(m)}$ denotes a random variable following Bernoulli distribution with the success probability $\mathbf{P}_{\mathcal{D}}(\alpha_m^*; \theta^*)$, and f_m is the probability function of $Y_1^{(m)}$.

Thus, Lemma 3 yields

$$\lim_{N \rightarrow \infty} \mathbf{E} [\exp(itA)] = \exp \left(-\frac{t^2}{2} \right). \quad (\text{D.26})$$

Therefore, $A \rightarrow \mathcal{N}(0, 1)$ holds.

Next, we consider the convergence of B . According to the Chebyshev inequality, for all $c > 0$ we obtain

$$P[|B - 1| > c] \leq \frac{\mathbf{E}[(B - 1)^2]}{c^2}. \quad (\text{D.27})$$

Here, $(B - 1)^2$ is upper bounded, and the expectation of $(B - 1)^2$ replacing $\mathbf{X}_M, \alpha_m \rightarrow \mathbf{Y}_M, \alpha_m^*$ also converges to 0 as follows. For simplicity, we define $W_m(Y^{(m)})$ and

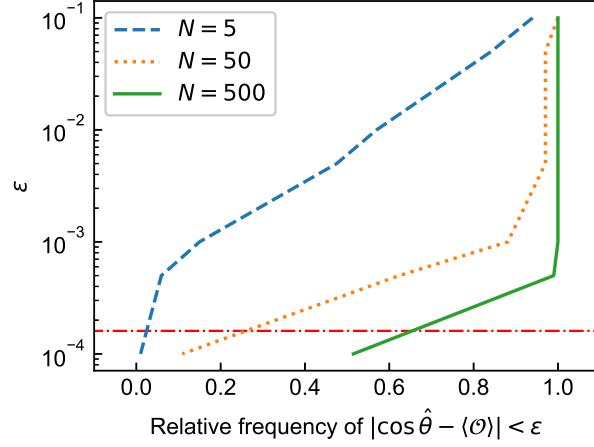


FIG. 6. The deviation of the maximum likelihood estimates from the true value. Here, we employed $\langle \mathcal{O} \rangle = 0.042$ and the same experimental settings in Section IV A. The plots represent the relative frequency in 100 trials that the estimate deviates from the true value less than ϵ . The horizontal line denotes the Cramér-Rao lower bound for $N = 500$.

$w_m(Y^{(m)})$ as

$$W_m(Y^{(m)}) := \partial_{\theta}^2 \ln F_m(Y^{(m)}; \alpha_m^*, \theta^*) - \mathbf{E} \left[\partial_{\theta}^2 \ln F_m(Y^{(m)}; \alpha_m^*, \theta^*) \right],$$

$$w_m(Y_1^{(m)}) := \partial_{\theta}^2 \ln f_m(Y_1^{(m)}; \alpha_m^*, \theta^*) - \mathbf{E} \left[\partial_{\theta}^2 \ln f_m(Y_1^{(m)}; \alpha_m^*, \theta^*) \right],$$

respectively.

$$\begin{aligned} & \mathbf{E} \left[(B-1)^2 \Big|_{\mathbf{X}_M, \alpha_m \rightarrow Y_M, \alpha_m^*} \right] \\ &= \frac{\mathbf{V} \left[\partial_{\theta}^2 \ln \prod_{m=1}^M F_m(Y^{(m)}; \alpha_m^*, \theta^*) \right]}{[\mathcal{I}_{c, \text{tot}}^*(\theta^*)]^2} \\ &= \frac{\sum_{n,m=1}^M \mathbf{E} [W_m(Y^{(m)}) W_n(Y^{(n)})]}{[\mathcal{I}_{c, \text{tot}}^*(\theta^*)]^2}, \\ &= \frac{N}{[\mathcal{I}_{c, \text{tot}}^*(\theta^*)]^2} \sum_{m=1}^M \mathbf{E} [w_m^2(Y_1^{(m)})], \\ &= \frac{1}{N} \frac{\sum_{m=1}^M \mathbf{E} [w_m^2(Y_1^{(m)})]}{\left[\sum_{m=1}^M \mathcal{I}_c(\alpha_m^*; \theta^*) \right]^2} \rightarrow 0, \end{aligned} \quad (\text{D.28})$$

where we used $\mathcal{I}_{c, \text{tot}}^*(\theta^*) = -\mathbf{E}[\partial_{\theta}^2 \ln \prod_{m=1}^M F_m]$ for the first equality. Thus, Lemma 3 establishes that $B \rightarrow 1$ holds.

Since $N^{-1} \partial_{\theta}^3 \ln \mathcal{L}_M(\theta'; \mathbf{x}_M)$ is also upper bounded, $\hat{\theta}_M - \theta^* \rightarrow 0$ yields $C \rightarrow 0$. To sum up the above asymptotic properties, we conclude that the following convergence holds

$$\sqrt{\mathcal{I}_{c, \text{tot}}^*(\theta^*)} (\hat{\theta}_M - \theta^*) \rightarrow \mathcal{N}(0, 1). \quad (\text{D.29})$$

In addition, delta method [20] yields more suitable expression:

$$\sqrt{\mathcal{I}_{c, \text{tot}}^*(\theta^*)} (\cos \hat{\theta}_M - \cos \theta^*) \rightarrow \mathcal{N}(0, \sin^2 \theta^*). \quad (\text{D.30})$$

□

To complete the proof of Theorem 2, we finally show the following lemma.

Lemma 3. *Let $h(\mathbf{x}_M, \alpha_2, \dots, \alpha_M)$ be an upper bounded function on $\mathbf{x}_M \in \{0, 1, \dots, N\}^M$ and $Y^{(m)}$ ($m = 1, 2, \dots, M$) be an independent random variable following Binomial distribution $\text{Bin}(N, \mathbf{P}_{\mathcal{D}}(\alpha_m^*; \theta^*))$. Suppose that $\mathbf{E}[h(\mathbf{Y}_M, \alpha_2^*, \dots, \alpha_M^*)]$ converges to some constant β as $N \rightarrow \infty$, then the following convergence holds*

$$\lim_{N \rightarrow \infty} \mathbf{E}[h(\mathbf{X}_M, \alpha_2(\mathbf{X}_1), \dots, \alpha_M(\mathbf{X}_{M-1}))] = \beta. \quad (\text{D.31})$$

Proof. Expanding the l.h.s. in Eq. (D.31), we obtain

$$\begin{aligned}
\mathbf{E} [h(\mathbf{X}_M, \alpha_2(\mathbf{X}_1), \dots, \alpha_M(\mathbf{X}_{M-1}))] &= \sum_{\mathbf{x}_M} \mathcal{L}_M(\mathbf{x}_M; \theta^*) h(\mathbf{x}_M, \alpha_2(\mathbf{x}_1), \dots, \alpha_M(\mathbf{x}_{M-1})) \\
&= \sum_{\substack{\mathbf{x}_M \\ \alpha_k(\mathbf{x}_{k-1}) = \alpha_k^* \forall k}} \mathcal{L}_M(\mathbf{x}_M; \theta^*) h(\mathbf{x}_M, \alpha_2(\mathbf{x}_1), \dots, \alpha_M(\mathbf{x}_{M-1})) \\
&\quad + \sum_{\substack{\mathbf{x}_M \\ \alpha_k(\mathbf{x}_{k-1}) \neq \alpha_k^* \exists k}} \mathcal{L}_M(\mathbf{x}_M; \theta^*) h(\mathbf{x}_M, \alpha_2(\mathbf{x}_1), \dots, \alpha_M(\mathbf{x}_{M-1})) \\
&= \sum_{\substack{\mathbf{x}_M \\ \alpha_k(\mathbf{x}_{k-1}) = \alpha_k^* \forall k}} \prod_{m=1}^M F_m(x^{(m)}; \alpha_m^*, \theta^*) h(\mathbf{x}_M, \alpha_2^*, \dots, \alpha_M^*) \\
&\quad + \sum_{\substack{\mathbf{x}_M \\ \alpha_k(\mathbf{x}_{k-1}) \neq \alpha_k^* \exists k}} \mathcal{L}_M(\mathbf{x}_M; \theta^*) h(\mathbf{x}_M, \alpha_2(\mathbf{x}_1), \dots, \alpha_M(\mathbf{x}_{M-1})) \\
&= \mathbf{E} [h(\mathbf{Y}_M, \alpha_2^*, \dots, \alpha_M^*)] \\
&\quad + \sum_{\substack{\mathbf{x}_M \\ \alpha_k(\mathbf{x}_{k-1}) \neq \alpha_k^* \exists k}} \mathcal{L}_M(\mathbf{x}_M; \theta^*) h(\mathbf{x}_M, \alpha_2(\mathbf{x}_1), \dots, \alpha_M(\mathbf{x}_{M-1})) \\
&\quad - \sum_{\substack{\mathbf{x}_M \\ \alpha_k(\mathbf{x}_{k-1}) \neq \alpha_k^* \exists k}} \prod_{m=1}^M F_m(x^{(m)}; \alpha_m^*, \theta^*) h(\mathbf{x}_M, \alpha_2^*, \dots, \alpha_M^*). \tag{D.32}
\end{aligned}$$

The above expression yields the following inequality

$$\begin{aligned}
&|\mathbf{E} [h(\mathbf{X}_M, \alpha_2(\mathbf{X}_1), \dots, \alpha_M(\mathbf{X}_{M-1}))] - \beta| \\
&\leq |\mathbf{E} [h(\mathbf{Y}_M, \alpha_2^*, \dots, \alpha_M^*)] - \beta| \\
&\quad + \sum_{\substack{\mathbf{x}_M \\ \alpha_k(\mathbf{x}_{k-1}) \neq \alpha_k^* \exists k}} \mathcal{L}_M(\mathbf{x}_M; \theta^*) |h(\mathbf{x}_M, \alpha_2(\mathbf{x}_1), \dots, \alpha_M(\mathbf{x}_{M-1}))| \\
&\quad + \sum_{\substack{\mathbf{x}_M \\ \alpha_k(\mathbf{x}_{k-1}) \neq \alpha_k^* \exists k}} \prod_{m=1}^M F_m(x^{(m)}; \alpha_m^*, \theta^*) |h(\mathbf{x}_M, \alpha_2^*, \dots, \alpha_M^*)| \\
&\leq |\mathbf{E} [h(\mathbf{Y}_M, \alpha_2^*, \dots, \alpha_M^*)] - \beta| + \gamma \sum_{\substack{\mathbf{x}_M \\ \alpha_k(\mathbf{x}_{k-1}) \neq \alpha_k^* \exists k}} \left(\mathcal{L}_M(\mathbf{x}_M; \theta^*) + \prod_{m=1}^M F_m(x^{(m)}; \alpha_m^*, \theta^*) \right), \tag{D.33}
\end{aligned}$$

where γ is the upper bound of h . The convergence of amplified levels implies that for all $\epsilon > 0$ there exists $N^* \in \mathbb{N}$ such that

$$P[\alpha_k(\mathbf{X}_{k-1}) = \alpha_k^* \forall k] = \sum_{\substack{\mathbf{x}_M \\ \alpha_k(\mathbf{x}_{k-1}) = \alpha_k^* \forall k}} \mathcal{L}_M(\mathbf{x}_M; \theta^*) = \sum_{\substack{\mathbf{x}_M \\ \alpha_k(\mathbf{x}_{k-1}) = \alpha_k^* \forall k}} \prod_{m=1}^M F_m(x^{(m)}; \alpha_m^*, \theta^*) > 1 - \frac{\epsilon}{2\gamma}, \tag{D.34}$$

for all $N > N^*$. Combining Eqs. (D.33), (D.34) and the assumption for the convergence of $\mathbf{E} [h(\mathbf{Y}_M, \alpha_2^*, \dots, \alpha_M^*)]$, we obtain Eq. (D.31). \square

E. Additional experiment

We provide additional results to confirm the asymptotic property of our estimator in more noisy setting.

Here, all settings except for the noise levels were equivalent to Section IV A, and the depolarization noise was set to $p_s = 1$ and $p_q = 0.90$. In Fig. 7, we can confirm that the RMSE achieves the CCR bound (also QCR bound) sufficiently in $N = 500$ as in Section IV A.

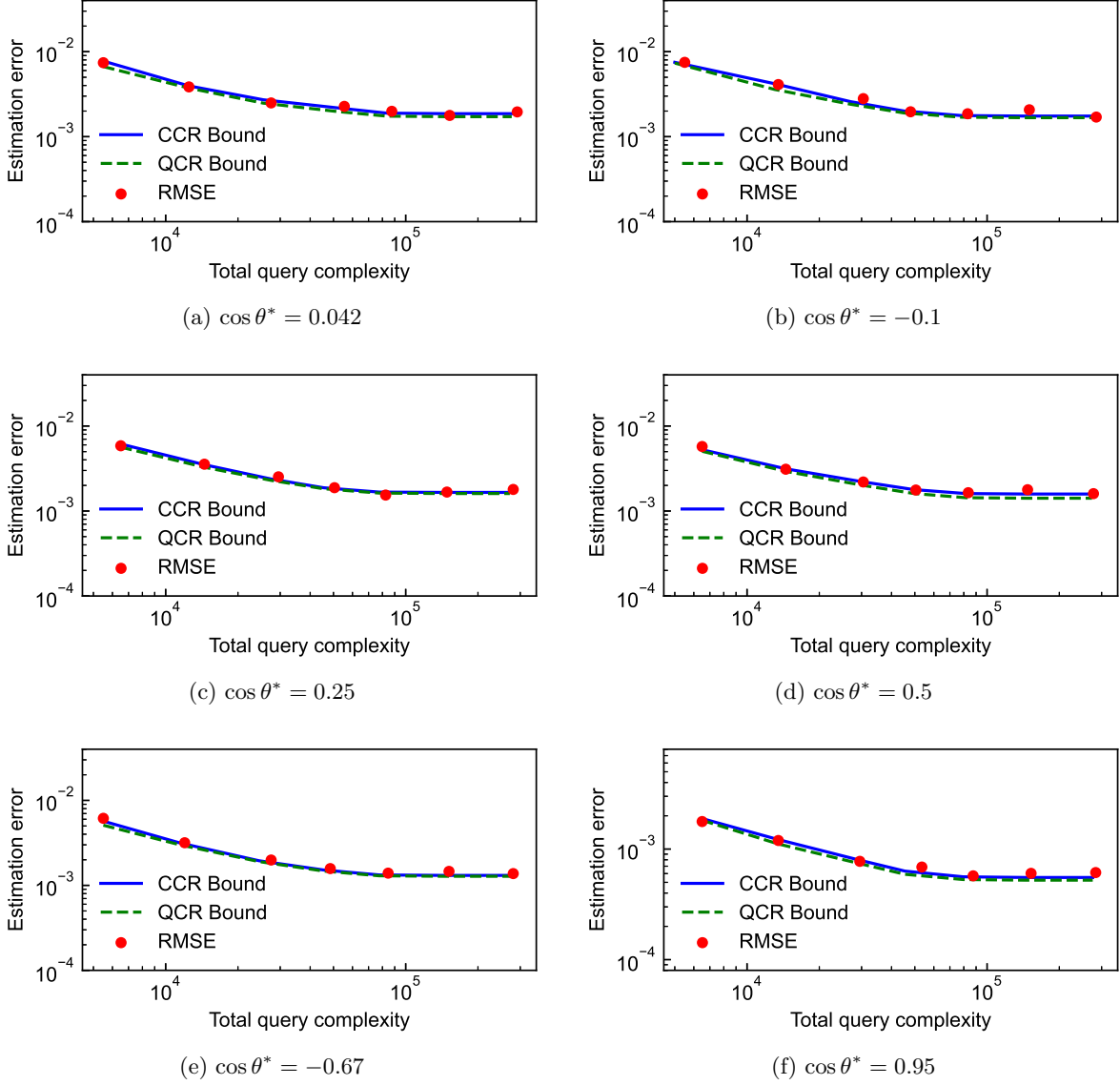


FIG. 7. The estimation error and the total query complexity for several target values. The root mean squared error (RMSE) of the estimator $\hat{\theta}$ was evaluated by 200 trials, and the plots correspond to $M = 3, 4, \dots, 9$ from left to right. Since the total number of queries is a random variable in our method, the RMSE was plotted as a function of the maximum value of the realized total number of queries. The blue solid line and green dashed line represent the asymptotic values of CCR/QCR bounds obtained from the corresponding classical/quantum Fisher information $\mathcal{I}_{c/q, \text{tot}}^*(\theta^*)$, respectively.